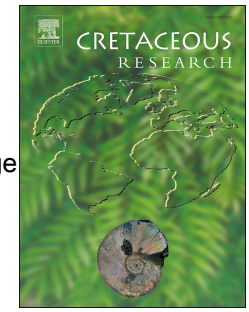

New Albian (Cretaceous) radiolarian age constraints for the Dumak ophiolitic mélange from the Shuru area, Eastern Iran

Péter Ozsvárt, Elham Bahramnejad, Sasan Bagheri, Mortaza Sharifi

PII: S0195-6671(19)30270-8

DOI: https://doi.org/10.1016/j.cretres.2020.104451

Reference: YCRES 104451

To appear in: *Cretaceous Research*

Received Date: 27 June 2019

Revised Date: 5 March 2020

Accepted Date: 8 March 2020

Please cite this article as: Ozsvárt, P., Bahramnejad, E., Bagheri, S., Sharifi, M., New Albian (Cretaceous) radiolarian age constraints for the Dumak ophiolitic mélange from the Shuru area, Eastern Iran, *Cretaceous Research*, https://doi.org/10.1016/j.cretres.2020.104451.

New Albian (Cretaceous) radiolarian age constraints for the Dumak ophiolitic mélange from the Shuru area, Eastern Iran

Péter Ozsvárt[1], Elham Bahramnejad[2], Sasan Bagheri[3], Mortaza Sharifi[2]

[1]MTA-MTM-ELTE, Research Group for Paleontology, P.O. BOX 137, 1431 Budapest, Hungary
[2]Department of Geology, Faculty of Sciences, University of Isfahan, Isfahan, Iran
[3]Department of Geology, Faculty of Sciences, University of Sistan and Baluchestan, Zahedan, Iran

Abstract

The Dumak ophiolitic mélange is part of the nearly complete Neh Ophiolite Complex in Eastern Iran. This complex exhibits a typical ophiolite suite that consists of mantle peridotite, cumulates, gabbro, sheeted dikes, pillow basalt and a sedimentary cover including pelagic and shallow-water deposits. A sequence of red radiolarites intercalated with mid-oceanic ridge-related basalt and pelagic limestone was examined from the Shuru part of the Dumak ophiolitic mélange. A relatively well-preserved and diverse radiolarian assemblage was extracted that includes 25 genera with 19 spumellarian and 26 nassellarian species. The radiolarian microfauna from the Shuru section provides the first biostratigraphical data which establishes a Cretaceous, middle Albian age for the ophiolitic mélange. The new age data contribute to a better understanding of the geodynamic evolution of the eastern branch of the Neotethys.

Keywords: Radiolaria, radiolarites, Neotethys, Neh Ophiolite Complex

1. Introduction

Understanding the geology of the collision zone in the Alpine-Himalayan orogenic belt is critical to reconstruct the evolution of the Neotethyan Ocean during Mesozoic-Cenozoic times (e.g. Agard et al., 2007, 2011). The western part of this zone (i.e. the Peri-Mediterranean Neotethys) has been extensively studied from a geodynamic aspect (e.g. Şengör et al., 1984; Robertson, 2002, 2004; Stampfli and Kozur, 2006; Bortolotti and Principi, 2005; Dilek et al., 2007, Schmid et al., 2008), but significantly fewer studies have focused on the eastern part (e.g. Tirrul et al., 1983, Stöcklin, 1977). The Sistan suture zone (SSZ) in Eastern Iran plays a key role in the geodynamic reconstruction of the long Neotethyan suture zone (Fig. 1). The nearly north-south-trending SSZ stretches for over 1000 km between the Lut block (Eastern Iran) and the Afghan block (Western Afghanistan). Tirrul et al. (1983) subdivided the SSZ into three main units: two ophiolitic-accretionary complexes (Neh and Ratuk) and the Sefidabeh forearc basin between them. The Neh accretionary complex contains blocks of various lithologies and ages, set in a sedimentary or volcano-sedimentary matrix (Maurizot, 1979; Tirrul et al., 1983). Commonly, these tectonic slices contain a thick succession of deep-water sediments (radiolarites) which are locally associated with ophiolite sequences. Any geodynamic model for the opening and closure processes needs to be based primarily on detailed biostratigraphic dating of these different tectonic slices. Fortunately, a well-preserved and relatively rich radiolarian fauna was extracted from a single radiolarite

sample in the Shuru area which is part of the Dumak ophiolitic mélange. Previously, only a few radiolarian records were reported from the SSZ (Soulabest region) by Babazadeh and De Wever (2004a, b) and Babazadeh (2007). The aim of this study is to present new radiolarian biostratigraphical age data and systematic paleontology from the SSZ in Eastern Iran where the radiolarite directly overlies basalts, therefore, the results allow an improved reconstruction of the evolution of the eastern branch of Neotethys from opening to closure during Mesozoic and early Cenozoic times.

2. Geological setting

The eastern Iranian range geologically corresponds to the Sistan suture zone (SSZ, Fig. 1). Folded Paleogene accretionary prisms and various Mesozoic ophiolitic assemblages are mixed in this zone. The main Neotethyan ophiolitic remnants in the SSZ from north to south are as follows: the Birjand ophiolite (Pang et al., 2012), the Nehbandan ophiolitic complex (Delavari et al., 2009; Saccani et al., 2010), the Tchehel Kureh ophiolite (Delaloye and Desmonse, 1980) and the Talkhab mélange complex (McCall, 1985, 2002). Formation and emplacement of these ophiolites reflect the consumption of the Sistan arm of Neotethys and subduction beneath the Afghan block (e.g. Agard et al., 2007, 2011; Saccani et al., 2010) and subsequent collision between the Lut and Afghan continental blocks during the late Paleogene (e.g. Tirrul et al., 1983). Subduction-related blueschists and eclogites associated with the Birjand ophiolites (Fotoohi Rad et al., 2005) provided early to late Cretaceous radiometric ages (Bröcker et al., 2010, 2013), and these high-pressure metamorphic rocks are unconformably overlain by Maastrichtian rudist-bearing limestone (Tirrul et al., 1983).

The Neh and Ratuk complexes have been considered as accretionary prisms and their overlying sediments attributed to the forearc Sefidabeh basin, developed at the frontal part of the Afghan block. The following suite of rocks is exposed there (after Tirrul et al., 1983): (1) ophiolites with lower Aptian to middle upper Albian and Cenomanian to Maastrichtian pelagic sedimentary rocks; (2) Upper Cretaceous–Eocene phyllites; and (3) Upper Cretaceous–Lower Eocene unmetamorphosed marine clastic sedimentary rocks including sandstone and marly turbidite. Detritus includes fragments of ophiolitic chert, basalt and gabbro. Sedimentary fill of the Sefidabeh basin includes Cenomanian to Eocene clastic deposits with deep-marine carbonates and calc-alkaline lavas (Camp and Griffis, 1982).

Radiolarites of the Ratuk complex, the only radiolarites studied so far in the SSZ, are characterized by two faunal assemblages of early Aptian and middle late Albian ages (Babazadeh and De Wever, 2004a, b), although deep-water sedimentation continued until the Early Eocene (Saccani et al., 2010).

2.1 Dumak ophiolitic mélange

The Dumak ophiolitic mélange is located on the western margin of the SSZ (Fig. 1). This mélange is part of the long ophiolitic belt which was emplaced in connection with the East Lut fault system that extends from Birjand to Iranshahr (Walker and Jackson, 2004). The elongate exposures of this mélange spread toward the north and south, to the ophiolites of Nosrat Abad and the Kurin, respectively. Despite the fact that some geological evidence such as the Eocene Lut magmatic arc (Arjmandzadeh et al., 2010) implies the subduction of the Sistan oceanic lithosphere under the Lut block (Pang et al., 2012), direct evidence for remnants of a westward-directed

subduction zone and associated high-pressure metamorphic rocks and accretionary prisms have not been reported so far. In addition, the nature of these ophiolites, their tectonic evolution, geological setting and temporal correlation have not been carefully reviewed in East Iran.

The upper part of the ophiolitic sequence in the Dumak ophiolitic mélange appears in a large-scale structural curvature known as the Shuru arc. Most of the pelagic sedimentary rocks overlying the ophiolite are found in this northward convex structure which separates the Eocene flysch-like sediments in the south from the main body of the Dumak mélange in the north. This arc is structurally composed of an imbricated thrust sequence which shows a southward regional transport direction (Fig. 2).

The upper part of the ophiolite that includes sheeted dikes, pillow basalt, and deep-water sediments extends along the flysch deposit and terrigenous sediments in the Shuru area (Fig. 2). A northeast-trending assemblage of sheeted dikes is accompanied by pillow basalts together with clay-rich sediments and radiolarite. In outcrop, these dikes are dark to light green in color and are generally aphyric and aphanitic. A considerable amount of red clay-rich pelagic sedimentary rocks is found along with the basaltic units in the Shuru area (Fig. 3). The bands of radiolarian cherts which are contained in a sequence of red pelagic clays comformably overlie the clays in the upper part of the sequence. The series continues with massive flysch-like turbidites of Eocene age (Fig. 3).

3. Materials and method

Samples were collected from diverse localities of the Dumak ophiolitic mélange by Elham Bahramnejad and −Sasan Bagheri. The sampled lithologies consist of slightly metamorphosed fine-grained sandstone with carbonate, limestone, limestone with chert and radiolarite. Only the Shu95-3 sample contains a rich, relatively well-preserved and diverse radiolarian fauna. This sample was collected from a sliced part of pelagic sediment overlying basalt and sheeted dikes. Approximately 350-500 g of dice-sized crushed chert from each sample was processed with the dissolution method. Samples were dried and placed in approx. 3–5% HF (nine parts distilled water and one part concentrated HF (48%) following standard laboratory procedures of Pessagno and Newport (1972). The residues were washed through a 50 μm sieve and dried. The laboratory preparation of the samples was carried out at the Hungarian Natural History Museum, Budapest. Photomicrographs of the radiolarians figured herein were taken using a Hitachi S-2600 N-type Scanning Electron Microscope at the Hungarian Natural History Museum, Budapest. The radiolarian specimens of the Dumak ophiolitic mélange are deposited in the Hungarian Natural History Museum in Budapest, Hungary.

4. Radiolarian fauna

The radiolarian assemblage from sample Shu 95-3 contains 19 determined spumellarian and 26 nassellarian species, assigned to 25 genera. Generally, each determined nassellarian species contains 10–15 specimens, whereas spumellarian species contain only one or two specimens. Four nassellarian genera (*Dictyomitra*, *Pseudodictyomitra*, *Hiscocapsa* and *Stichomitra*) dominate the radiolarian assemblage, although *Acaeniotyle* spp. and *Archaeospongoprunum cortinaense* are also relatively abundant in the radiolarian fauna. The assemblage contains some extremely long-ranging species such as *Archaeocenosphaera clathrata* (Parona, 1890) and *Acanthocircus levis* (Donofrio and Mostler, 1978). Other species are also known to have a long range,

such as *Acaeniotyle diaphorogona* Foreman, 1973, *Acaeniotyle umbilicata* (Rüst, 1898) and *Crucella messinae* Pessagno, 1971. The following typical Barremian to Cenomanian or Turonian radiolarians are important members of the assemblage: *Dictyomitra communis* (Squinabol, 1904), *Dictyomitra montisserei* (Squinabol, 1903), *Obeliscoites perspicuus* (Squinabol, 1903), *Xitus mclaughlini* (Pessagno, 1977b), *Crococapsa asseni* (Tan, 1927) and *Hiscocapsa grutterinki* (Tan, 1927). The sample also contains typical Aptian to Turonian (or younger) radiolarians such as *Crucella euganea* (Squinabol, 1903), *Napora crassispina* (Squinabol, 1903), *Pseudodictyomitra lodogaensis* Pessagno, 1977b and *Parvimitrella communis* (Squinabol, 1903). The biostratigraphically most important species are the short-ranging (dominantly from Albian or Albian to Cenomanian) forms such as *Dactyliodiscus cayeuxi* Squinabol, 1903, *Thanarla brouweri* (Tan, 1927), *Dictyomitra obesa* (Squinabol, 1903), *Xitus spinosus* (Squinabol, 1904), *Parvimitrella magna* Squinabol, 1904 and *Dorypyle communis* (Squinabol, 1903). Based on the presence of *Thanarla brouweri* (Tan, 1927), *Dictyomitra obesa* (Squinabol, 1903), *Xitus spinosus* (Squinabol, 1904), *Parvimitrella magna* (Squinabol, 1904), and *Dorypyle communis* (Squinabol, 1903), this assemblage is assigned to the Albian (Romanus and Missilis radiolarian subzones of the Spoletoensis Zone, which comprises UA 10–13 of O'Dogherty, 1994). A more precise biostratigraphic age assignment is possible to the late middle to early late Albian (early Missilis radiolarian subzone which allows correlation to UA 12 of O'Dogherty, 1994) based on the co-occurrence of *Dictyomitra obesa* (Squinabol, 1903), *Parvimitrella magna* (Squinabol, 1904) *Acanthocircus multidentatus* (Squinabol, 1914) and *Acanthocircus levis* (Donofrio and Mostler, 1978). However, *Hiscocapsa grutterinki* (Tan, 1927), *Thanarla brouweri* (Tan, 1927) and *Crococapsa asseni* (Tan, 1927) disappear from the fossil record after the Romanus subzone, therefore the sample Shu 95-3 most probably represents the Romanus and Missilis subzones (O'Dogherty, 1994). Detailed range data of the species in the studied sample from the Shuru section are presented in Fig. 4.

4.1 Systematic paleontology

Class Radiolaria Müller, 1858

Subclass Polycystina Ehrenberg 1838 emend. Riedel, 1967

Order Spumellaria Ehrenberg, 1875

Family Xiphostylidae Haeckel, 1881

Genus *Archaeocenosphaera* Pessagno and Yang, 1989 in Pessagno et al., 1989

Type species: *Archaeocenosphaera ruesti* Pessagno and Yang, 1989 in Pessagno et al., 1989

Archaeocenosphaera clathrata (Parona, 1890)

Fig. 5.1

1880? *Heliosphaera echinoidites* n. sp.: Pantanelli, p. 46, fig. 8.

1890 *Cenosphaera clathrata* n. sp.: Parona, p. 19, pl. I, fig. 5.

2015 *Archaeocenosphaera clathrata* (Parona): Ozsvárt et al., p. 344, fig. 5.1. (cum syn.)

Remarks: *A. clathrata* (Parona) is clearly distinguished from other species of the genus *Archaeocenosphaera* by the hexagonal shape of pores, but this specimen from the Neh accretionary complex, Iran has smaller sized pores.

Range: lower Devonian – Eocene.

Occurrence: Cosmopolitan.

Family Acaeniotylinae Yang, 1993

Genus Acaeniotyle Foreman, 1973

Type species: *Xiphosphaera umbilicata* (Rüst, 1898)

Acaeniotyle diaphorogona Foreman, 1973

Fig. 5.2

1973 *Acaeniotyle diaphorogona* n. sp.: Foreman, p. 258, pl. 2, figs. 2-5.

1993 *Acastea acer* n. sp.: Yang, p. 94, pl. 15, figs. 1-2, 13, 15, 16; pl. 16, figs. 3, 8, 14.

1994 *Acaeniotyle diaphorogona* Foreman: O'Dogherty, p. 284, pl. 50, figs. 8-11. (cum syn.)

1995 *Acaeniotyle diaphorogona* gr. Foreman: Baumgartner et al., p. 54, pl. 3090, figs. 1-6.

1997 *Acastea tenuis* n. sp.: Hull, p. 35, pl. 10, figs. 8-10, 15, 22.

1998 *Acastea diaphorogona* (Foreman): Matsuoka, pl. 13, fig. 197.

2004 *Acaeniotyle diaphorogona* Foreman: Bragina, p. 398, pl. 17, fig. 4; pl. 41, figs. 7, 16.

2005 *Acaeniotyle diaphorogona* Foreman: Vishnevskaya et al., pl. 2, fig. 14.2007 *Acaeniotyle diaphorogona* Foreman: Danelian et al., pl. 3, fig. 2.

2011 *Acaeniotyle diaphorogona* Foreman: Zyabrev, pl. 1, fig.

2011 *Acaeniotyle diaphorogona* Foreman: Bandini et al., pl. 2, fig. 7.

2017 *Acaeniotyle* sp. cf. *A. diaphorogona* Foreman: Xu and Luo, fig. 3F.

Remarks: This fragmentary specimen is assigned to the genus *Acaeniotyle*, based on its characteristic shell with large porous nodes. This specimen differs from the holotype of *A. diaphorogona* Foreman by fewer pores on its nodes. Generally, one node contains 6-9 rounded pores, but this specimen bears 3-5 pores on each node.

Range: upper Bajocian – lower Turonian (Baumgartner et al., 1995, O'Dogherty, 1994 and Bragina et al., 2007).

Occurrence: Cosmopolitan.

Acaeniotyle umbilicata (Rüst, 1898)

Figs. 5.3-4

1898 *Xiphosphaera umbilicata* n. sp.: Rüst, p. 7, pl. I, fig. 9.

1994 *Acaeniotyle umbilicata* (Rüst): O'Dogherty, p.289, pl. 51, figs. 19-20. (cum syn.)

1995 *Acaeniotyle umbilicata* (Rüst): Baumgartner et al., p. 54, pl. 3092, figs. 1-7.

1997 *Acaeniotyle umbilicata* (Rüst): Dumitrica et al., p. 21, pl. 2, fig. 1.

2003 *Acaeniotyle umbilicata* (Rüst): Ziabrev et al., fig. 3.1

2004 *Acaeniotyle umbilicata* (Rüst): Bragina, p. 401, pl. 17, figs. 3 and 7; pl. 41, fig. 8.
2005 *Acaeniotyle umbilicata* (Rüst): Vishnevskaya et al., pl. 2, fig. 5.
2009 *Acaeniotyle umbilicata* (Rüst): Ishii et al., pl. 1, fig. 2.
2011 *Acaeniotyle umbilicata* (Rüst): Zyabrev, pl. 1, fig. 4.
2013 *Acaeniotyle umbilicata* (Rüst): Zyabrev and Anoikin, pl. fig. 2.

Remarks: These specimens from the Neh accretionary complex, Iran resemble the holotype, although the illustrated specimen in Fig. 5.3 has shorter and slightly more robust polar spines with significantly wider grooves between ridges than the illustrated specimen by Rüst (1898).
Range: upper Oxfordian – upper Campanian (Baumgartner et al., 1995, Bragina and Bragin, 2004, Górka, 1989).
Occurrence: Cosmopolitan.

Acaeniotyle sp. cf. *A.* sp. A. sensu Thurow, 1988
Fig. 5.5

1988 *Acaeniotyle* sp. A.: Thurow, p. 396, pl. 6, fig. 2.
1994 *Acaeniotyle amplissima* (Foreman): O'Dogherty, p. 288, pl. 51, figs. 11-14.
1998 *Acaeniotyle* (?) *glebulosa* (Foreman): Salvini and Marcucci Passerini, fig. 6a.
2013 *Acaeniotyle amplissima* (Foreman): Bragina and Bragin, pl. 1, fig. 4.
2015 *Acaeniotyle amplissima* (Foreman): Shirdashtzadeh et al., fig. 4.14.
2015 *Acaeniotyle amplissima* (Foreman): Bragina and Bragin, pl. 2, fig. 6.

Remarks: This specimen is closely related to *Acaeniotyle* sp. A. (Thurow, 1988), but not in the least related to *Staurosphaera amplissima* Foreman (1973) which has no characteristic large nodes on surface. Nodes of the illustrated specimen contain fewer pores (3-4) and they are slightly pointed.
Occurrence: Cosmopolitan.

Family Intermediellidae Lahm, 1984
Genus *Tetrapaurinella* Kozur and Mostler, 1994
Tape species: *Tetrapaurinella discoidalis* Kozur and Mostler, 1994

Tetrapaurinella sp. 1
Figs. 5.6-8

1975 Actinommids gen. and sp. indet: Foreman, p. 33, pl. 2F, figs. 13-14.

Remarks: Poorly preserved specimens with a spongy and angular test. 4 needle-like, long and smooth, slightly curved spines. These specimens are identical with some of the illustrated Actinommids gen. and sp. indet by Foreman from 1975. Also reported similar form (*T. staurus* Dumitrica, 1997) of the upper Valanginian:

Hauterivian of the Fayah unit in Masirah ophiolite of Oman by Dumitrica et al., 1997, but that species has relatively shorter and straight spines.

Occurrence: Neh accretionary complex, Iran.

Tetrapaurinella sp. cf. *T. staurus* Dumitrica, 1997

Fig. 5.9

1997 *Tetrapaurinella staurus* n. sp.: Dumitrica in Dumitrica et al., p. 25, pl. 3, figs, 1-2.

2004a *Pseudoaulophacus* sp.: Babazadeh and De Wever, p. 203, Figs. 8F-G.

Remarks: This specimen bears few, short needle-like secondary spines on the test between main spines. However, the illustrated specimens of *T. staurus* Dumitrica do not bear secondary spines on the test, although it was mentioned in the description. Babazadeh and De Wever (2004a) illustrated a poorly preserved but very similar species as *Pseudoaulophacus* sp. from the Sistan Suture zone (Soulabest village) and Jud (1994) also published a very similar species as *Stylospongia* from the Hauterivian-Barremian section of the Apennines (Umbria), although this latter bears polar spines.

Occurrence: Neh accretionary complex, Iran.

Family Hagiastridae Riedel, 1971

Genus *Crucella* Pesssagno, 1971

Type species: *Crucella messinae* Pessagno, 1971

Crucella euganea (Squinabol, 1903)

Fig. 5.10

1903 *Stauralastrum euganeum* n. sp.: Squinabol, p. 123, pl. 9, fig. 19.

1994 *Crucella euganea* (Squinabol): O'Dogherty, p. 367, pl. 70, figs. 10-20. (cum syn.)

1998 *Crucella euganea* (Squinabol): Salvini and Marcucci, fig. 9.l.

2008 *Crucella euganea* (Squinabol): Zyabrev et al., fig. 6.9.

2016 *Crucella euganea* (Squinabol): Bragina and Bragin, pl. 4, fig. 4.

Remarks: However, three rays are broken off on the illustrated specimen, it can be specified to the *C. euganea* (Squinabol, 1903) because *C. euganea* (Squinabol, 1903) has a very characteristic, long, three-bladed and a slightly curved terminal spine.

Range: Aptian – Turonian (O'Dogherty, 1994).

Occurrence: Cosmopolitan.

Crucella sp. 1

Fig. 5.11

1971 *Crucella messinae* n. sp.: Pessagno, p. 56, pl. 6, figs. 1–3.

Remarks: Poorly preserved specimens with characteristic meshwork with large circular pores, although it resembles the Cenomanian *C. messinae* Pessagno, 1971, but cannot be specified, obviously.
Occurrence: Cosmopolitan.

Crucella sp. 2

Fig. 5.12

Remarks: Broken specimen wears four rays with rectangular pore frames arranged in double linear rows. Rows converge in slightly elevated ridges.
Occurrence: Neh accretionary complex, Iran.

Family Angulobracchiidae Baumgartner, 1980
Genus *Paronaella* Pessagno, 1971
Type species: *Paronaella solanoensis* Pessagno, 1971

Paronaella sp. cf. *P. communis* (Squinabol, 1903)

Fig. 5.13

cf. 1903 *Spongotripus communis* n. sp.: Squinabol, p. 123, pl. 9, fig. 7.
cf. 1989 *Pseudoaulophacus polonicus* n. sp.: Górka, p. 337, pl. 10, figs. 1-4.
cf. 1994 *Paronaella communis* (Squinabol): O'Dogherty, p. 353, pl. 66, figs. 9-16.

Remarks: Small, three-rayed form (one of them is absent) with long, three-bladed spines. Triangular outline similar to *P. communis* (Squinabol, 1903), but the test has been completely recrystallized. Górka (1989) published very similar specimens as *Pseudoaulophacus polonicus* n. sp., from the Campanian of Poland, but all spines are almost covered by the spongy outer layer of the test.
Occurrence: Neh accretionary complex, Iran.

Family Patulibracchiidae Pessagno, 1971
Genus *Halesium* Pessagno, 1971
Type species: *Halesium sexangulum* Pessagno, 1971

Halesium sp. cf. *H. nevianii* (Squinabol, 1903)

Figs. 5.14

cf. *Halesium nevianii* n. sp.: Squinabol, p. 122, pl. 10, fig. 6.
cf. *Halesium nevianii* Squinabol: O'Dogherty, p. 348, pl. 64, figs.19-24.

Remarks: The illustrated specimens with double rows of triangular pore frames with characteristic nodes and median bars. These specimens are similar to *H. nevianii* (Squinabol, 1903) but the preservation is fairly poor.
Occurrence: Neh accretionary complex, Iran.

Halesium sp. cf. *H. crassum* (Ozvoldová, 1979)
Figs. 5.15-16

cf. 1979 *Dictyastrum crassum* n. sp.: Ozvoldová, p. 10, pl. 2, figs. 1, 3.
cf. 1994 *Halesium nevianii* Squinabol: O'Dogherty, p. 348, pl. 64, figs. 17-18.

Remarks: Rays are more or less tetragonal in cross-section with characteristic central and lateral beams with large nodes at both rows. Nodes are connected by diagonal tiny bars that form triangular pore frames with relatively large pores. Rays broaden distally and terminate relatively large nodes that tapered distally. Large terminal nodes bear two thick lateral spines.
Occurrence: Neh accretionary complex, Iran.

Family Spongodiscidae Haeckel, 1862
Genus *Archaeospongoprunum* Pessagno, 1973
Type species: *Archaeospongoprunum venadoensis* Pessagno, 1973

Archaeospongoprunum cortinaense Pessagno, 1973
Figs. 6.1-2

1973 *Archaeospongoprunum cortinaensis* n. sp.: Pessagno, p. 60, pl. 9, figs. 4-6.
1989 *Archaeospongoprunum cortinaensis* Pessagno: Górka, p. 339, pl. 12, fig. 6, non 5.
non 1998 *Archaeospongoprunum cortinaensis* Pessagno: Salvini and Marcucci Passerini, fig. 9b.
2001 *Archaeospongoprunum* spp.: Snoke and Noble, fig. 5.9
2004 *Archaeospongoprunum cortinaensis* Pessagno: Bragina, p. 407, pl. 18, figs. 5, 11, 13, non 10, 14.
2004 *Archaeospongoprunum klingi* Pessagno, 1977: Bragina, p. 407, pl. 18, fig. 12.
2006 *Archaeospongoprunum cortinaensis* Pessagno: Musavu-Moussavou and Danelian, p. 159, pl. 3, fig. 15, non 11-14.
non 2007 *Archaeospongoprunum cortinaensis* Pessagno: Musavu-Moussavou et al., pl. 5, figs. 3-6.
2009 *Archaeospongoprunum cortinaensis* Pessagno: Bragina, pl. 2, figs. 3-5.

Remarks: Secondary grooves on the ridges of spines are somewhat wider and deeper than on illustrated holotype by Pessagno (1973).
Range: Berriasian (Kiessling, 1995) – Campanian (Górka, 1989).
Occurrence: Cosmopolitan.

Family Pseudoaulophacidae Riedel, 1967

Genus *Becus* Wu, 1986

Type species: *Becus gemmatus* Wu, 1986

Becus sp. cf. *B. gemmatus* Wu, 1986

Fig. 6.3, 7

cf. 1986 *Becus gemmatus* n. sp.: Wu, p. 356, pl. 1, figs., 14, 17, 18, 21.

cf. 1994 *Becus gemmatus* Wu: O'Dogherty, p. 317, pl. 58, figs. 4-8.

Remarks: This poorly preserved specimen figured herein possesses large nodes at the central part of the test and numerous, smooth pointed secondary spines.

Occurrence: Cosmopolitan.

Genus *Dactyliodiscus* Squinabol, 1904

Type species: *Dactyliodiscus cayeuxi* Squinabol, 1904

Dactyliodiscus cayeuxi Squinabol, 1903

Figs. 6.4-5

1903 *Dactyliodiscus Cayeuxi* n. sp.: Squinabol, p. 120, pl. 9, figs.18, 18a

1994 *Dactyliodiscus cayeuxi* Squinabol: O'Dogherty, p. 332, pl. 61, figs. 16-23. (cum syn.)

2011 *Dactyliodiscus cayeuxi* Squinabol: Zyabrev, pl. 1, fig. 17.

2015 *Dactyliodiscus cayeuxi* Squinabol: Bragina and Bragin, pl. 4, fig. 1.

Remarks: This poorly preserved specimen figured here has only two spines, the others broken, but the base of the discoidal test can be assigned to the *Dactyliodiscus cayeuxi* Squinabol, 1903.

Range: lower Albian – Cenomanian (O'Dogherty, 1994).

Occurrence: Western Neotethys.

Dactyliodiscus sp. cf. *D. longispinus* (Squinabol, 1904)

Fig. 6.6

cf. 1904 *Stylotrochus longispina* n. sp.: Squinabol, p. 207, pl. 6, fig. 8.

cf. 1904 *Spongolonche diversispina* n. sp.: Squinabol, p. 206, pl. 6, fig. 6.

cf. 1904 *Stylotrochus euganeus* n. sp.: Squinabol, p. 207, pl. 6, fig. 9.

cf. 1994 *Dactyliodiscus longispinus* (Squinabol): O'Dogherty, p. 333, pl. 62, figs. 6-11.

cf. 2004 *Dactyliodiscus longispinus* (Squinabol): Bragina, p. 431, pl. 26, figs. 4–13, pl. 27, fig. 1, pl. 38, figs. 4, 7, pl. 41, fig. 10.

cf. 2016 *Dactyliodiscus longispinus* (Squinabol): Bragina and Bragin, p. 318, pl. 3, figs. 1-2.

Remarks: This specimen differs from the illustrated holotype of *Stylotrochus longispina* Squinabol by having longer and slightly curved spines.

Occurrence: Western Neotethys.

Family Saturnalidae Deflandre, 1953

Genus *Mesosaturnalis* Kozur and Mostler, 1981

Type species: *Paleosaturnalis levis* Donofrio and Mostler, 1978

Acanthocircus levis (Donofrio and Mostler, 1978)

Figs 6.8-9

1914 *Saturnalis polymorphus* n. sp.: Squinabol, p. 293, pl. 22, figs. 12 non fig. 11; pl. 24, figs. 2-3. non figs. 4-7.

1978 *Paleosaturnalis levis* n. sp.: Donofrio and Mostler, p. 36, pl. 2, figs. 1-2.

1994 *Acanthocircus levis* (Donofrio and Mostler): O'Dogherty, p.251, pl. 43, figs. 5-7. (cum syn.)

2000 *Acanthocircus levis* (Donofrio and Mostler): Jasin, pl. 2, fig. 1

2015 *Acanthocircus levis* (Donofrio and Mostler): Shirdashtzadeh et al., fig. 5.17.

Range: Berriasian – middle Albian (Ishii et al., 2009 and O'Dogherty, 1994).

Occurrence: Western Neotethys.

Acanthocircus multidentatus (Squinabol, 1914)

Fig. 6.10

1914 *Saturnalis multidentatus* n. sp.: Squinabol, p. 298, pl. 23, figs. 11-12.

1994 *Acanthocircus multidentatus* (Squinabol): O'Dogherty, p.255, pl. 44, figs. 7-10. (cum syn.)

2000 *Acanthocircus multidentatus* (Squinabol): Jasin, pl. 2, fig. 2.

2004 *Acanthocircus multidentatus* (Squinabol): Bragina, p. 447, pl. 34, figs. 9, 12.

Remarks: *A. multidentatus* (Squinabol, 1914) differs from *A. levis* (Donofrio and Mostler, 1978) by having inner carina on the ring which is clearly recognizable in the illustrated specimen.

Range: middle Albian –Turonian (O'Dogherty, 1994).

Occurrence: Western Neotethys.

Order Nassellaria Ehrenberg, 1875

Family Ultranaporidae Pessagno, 1977b

Genus *Napora* Pessagno, 1977a

Type species: *Napora bukryi* Pessagno 1977a

Napora crassispina (Squinabol, 1903)

Figs. 6.11-12

1903 *Lychnocanium crassispina* n. sp.: Squinabol, p. 129, pl. 8, fig. 33.
1994 *Ultranapora crassispina* (Squinabol): O'Dogherty, p. 242, pl. 42, figs. 1-5. (cum syn.)
2013 *Ultranapora crassispina* (Squinabol): Bragina and Bragin, pl. 4, fig. 5.

Remarks: The specimen figured herein has a slightly skew apical horn with deep grooves. Cephalis poreless, spherical and smooth.
Range: Aptian – lower Cenomanian (O'Dogherty, 1994).
Occurrence: Western Neotethys and South India.

Napora sp.

Figs. 6.13-14

Remarks: Preservation is very poor, therefore we cannot assign this form to species level.. Apical horn similar to *N. praespinifera* Pessagno, but cephalis and thorax much smaller and less inflated.
Occurrence: Neh accretionary complex, Iran.

Family Neosciadiocapsidae Pessagno, 1969
Genus *Sciadiocapsa* Squinabol, 1904
Type species: *Sciadiocapsa euganea* Squinabol, 1904

Sciadiocapsa sp.

Fig. 6.15

Remarks: Absence of apical horn suggests this form more likely belongs to the genus *Sciadiocapsa.*
Occurrence: Neh accretionary complex, Iran.

Family Archaeodictyomitridae Pessagno, 1976
Genus *Archaeodictyomitra* Pessagno, 1976
Type species: *Archaeodictyomitra squinaboli* Pessagno, 1976

Archaeodictyomitra chalilovi (Aliev, 1965)

Fig. 6.16

1965 *Lithocampe chalilovi* n. sp.: Aliev, p. 66, pl. 12, figs. 10-13.
pars 1994 *Dictyomitra gracilis* (Squinabol): O'Dogherty, p. 73, pl. 1, figs. 16, 21, 23.
1994 *Archaeodictyomitra chalilovi* (Aliev): Jud, p. 63, pl. 3, figs. 12-14. (cum syn.)
2015 *Dictyomitra montisserei* (Squinabol): Shirdashtzadeh et al., fig. 3.7-9

Remarks: The preservation is rather poor but this specimen was assigned to *A. chalilovi* (Aliev), although its distal pores are slightly bigger and its wall is rather massive. O'Dogherty illustrated more specimens of *Dictyomitra gracilis* (Squinabol) in 1904, although part of that series (pl. 1, figs. 16, 21, 23.) can be rather assigned to *A. chalilovi* (Aliev, 1965) thank s to the non-lobate outline.

Range: upper Hauterivian-?Barremian (Jud, 1994) – Albian (Asis and Jasin, 2012).

Occurrence: Cosmopolitan.

Archaeodictyomitra vulgaris Pessagno, 1977b

Figs. 6.17-18

1977b *Archaeodictyomitra vulgaris* n. sp.: Pessagno, p. 44, pl. 6, fig. 15.

1991 *Archaeodictyomitra vulgaris* Pessagno: Basov and Vishnevskaya, p. 171, pl. 18, figs. 1,4.

1996 *Archaeodictyomitra vulgaris* Pessagno: Zyabrev, pl. 1, fig. 4.

non 2004 *Archaeodictyomitra vulgaris* Pessagno: Bragina, p. 375, pl. 33, fig. 18.

2001 *Archaeodictyomitra vulgaris* Pessagno: Vishnevskaya, pl. 86, figs. 1,4; pl. 116, fig. 7.

2005 *Archaeodictyomitra vulgaris* Pessagno: Vishnevskaya et al., pl. 2, fig. 27.

2008 *Archaeodictyomitra vulgaris* Pessagno: Danelian, p. 5, pl. 1, fig. 3; pl. 2, figs. 11-12. (cum syn.)

2009 *Archaeodictyomitra vulgaris* Pessagno: Kurogi and Takahashi, pl. 1, fig. 17.

2013 *Archaeodictyomitra montisserei* (Squinabol): Bragina and Bragin, pl. 3, figs. 12-13.

Remarks: Test more rounded distally and somewhat more perfectly conical than the holotype, costae are sharper and elevated higher and it bears bigger pores.

Range: upper Valanginian –lower Turonian, but probably this species already appeared in the late Jurassic as Hull (1997) reported a similar (*Archaeodictyomitra* sp. cf. *A. vulgaris* Pessagno) specimen from Tithonian of California (Stanley Mountain).

Occurrence: Cosmopolitan.

Genus *Thanarla* Pessagno, 1977b

Type species: *Phormocyrtis veneta* Squinabol, 1903

Thanarla brouweri (Tan, 1927)

Fig. 6.19

1927 *Eucyrtidium Brouweri* n. sp.: Tan, p. 58, pl. 11, figs. 89a-b.

1994 *Thanarla brouweri* (Tan): O'Dogherty, p. 86, pl. 5, figs. 1-12. (cum syn.)

2003 *Thanarla brouweri* (Tan): Ziabrev et al., fig. 3.43.

2008 *Thanarla brouweri* (Tan): Danelian, pl. 1, figs, 7-9; pl. 2, figs. 15-18; pl. 3, fig. 10. (cum syn.)

2008 *Thanarla brouweri* (Tan): Zyabrev et al., fig. 5.30.

2011 *Thanarla brouweri* (Tan): Zyabrev, pl. 3, fig. 20.

2011 *Thanarla brouweri* (Tan): Kurilov, Vishnevskaya, pl. 4, fig. 7.

2013 *Thanarla brouweri* (Tan): Zyabrev and Anoikin, pl, fig. 37.

2015 *Thanarla brouweri* (Tan): Zyabrev et al., fig. 4.7.

Range: upper Barremian – middle Albian (O'Dogherty, 1994).

Occurrence: Cosmopolitan.

Genus *Dictyomitra* Zittel, 1876

Type species: *Dictyomitra multicostata* Zittel, 1876

Dictyomitra gracilis (Squinabol, 1903)

Figs. 7.1-2

1903 *Sethoconus gracilis* n. sp.: Squinabol, p. 131, pl. 10, fig. 13

pars 1994 *Dictyomitra gracilis* (Squinabol): O'Dogherty, p. 73, pl. 1, figs. 15, 17, 22, 24.

2008 *Mita gracilis* (Squinabol): Danelian, p. 6, pl. 3, figs. 8-9. (cum syn.)

2016 *Mita gracilis* (Squinabol): Bragina and Bragin, p. 333, pl. 6, figs. 1-2. (cum syn.)

Remarks: Due to the diagenetic alterations and recrystallization test poorly preserved, although it has hardly visible apical horn.

Range: The first appearance of *Dictyomitra gracilis* (Squinabol, 1903) can be observed within oceanic anoxic event OAE Ib (Erbacher and Thurow, 1997) in early Albian (in Romanus subzone after O'Dogherty, 1994) – Campanian (Urquhart, 1994).

Occurrence: Cosmopolitan.

Dictyomitra montisserei (Squinabol, 1903)

Figs. 7.3-5

1903 *Stichophormis Montis Serei* n. sp.: Squinabol, p. 137, pl. 8, fig. 38.

1994 *Dictyomitra montisserei* (Squinabol): O'Dogherty 1994, p. 77, pl. 3, figs 1-29. 8 (cum syn.)

2004a *Dictyomitra montisserei* (Squinabol): Babazadeh and De Wever, p. 195, Figs 6I-N; 7F.

2005 *Dictyomitra montisserei* (Squinabol): Vishnevskaya et al., pl. 3, fig. 9; pl. 4, fig. 15.

2007 *Archaeodictyomitra montisserei* (Squinabol): Musavu-Moussavou et al., p. 265, pl. 2, fig. 3. (cum syn.)

2008 *Archaeodictyomitra montisserei* (Squinabol): Danelian, p. 5, pl. 1, fig. 2; pl. 2, figs. 9-10; pl. 3, figs. 1-2. (cum syn.)

2011 *Archaeodictyomitra montisserei* (Squinabol): Bandini et al., pl. 11, fig. 2.

2012 *Dictyomitra montisserei* (Squinabol): Asis and Jasin, pl. 1, fig. 3.

2015 *Archaeodictyomitra montisserei* (Squinabol): Zyabrev et al., Fig 4.3.

2016 *Dictyomitra montisserei* (Squinabol): Kopaevich and Vishnevskaya, Fig. 8, t.

Range: middle Albian (O'Dogherty, 1994) – Turonian (Smrečková, 2011).

Occurrence: Cosmopolitan.

Dictyomitra obesa (Squinabol, 1903)

Figs. 7.6-8

1903 *Artophormis obesa* n. sp.: Squinabol, p. 137, pl. 10, fig. 1.

1994 *Dictyomitra obesa* (Squinabol): O'Dogherty, p. 74, pl. 2, figs. 2-6. (cum syn.)

2010 *Mita obesa* (Squinabol): Robin et al., fig. 5. 15.

2016 *Dictyomitra obesa* (Squinabol): Bragina and Bragin, p. 23, pl. 6, fig. 3. (cum syn.)

Remarks: *D. obesa* (Squinabol, 1903) has an asymmetrical test that is clearly recognizable in Figures 6.6 and 6.8, but it is not visible well in Figure 6.7 because it is front view.

Range: middle Albian – lower Cenomanian (O'Dogherty, 1994).

Occurrence: Cosmopolitan

Dictyomitra sp. cf. *D. obesa* (Squinabol, 1903)

Fig. 7.9

Remarks: This specimen is characterized by asymmetrical test, but it differs from *D. obesa* by well-developed strictures between chambers.

Occurrence: Neh accretionary complex, Iran.

Family Obeliscoitidae O'Dogherty, 1994

Genus *Obeliscoites* O'Dogherty, 1994

Type species: *Cyrtocapsa turris* Squinabol, 1903

Obeliscoites perspicuus (Squinabol, 1903)

Fig. 7.12

1903 *Cyrtocapsa perspicua* n. sp.: Squinabol, p. 142, pl. 10, fig. 16.

1994 *Obeliscoites perspicuus* (Squinabol): O'Dogherty, p. 191, pl. 29, figs. 5-18. (cum syn.)

2003 *Obeliscoites perspicuus* (Squinabol): Ziabrev et al., fig. 3.28.

2009 *Obeliscoites perspicuus* (Squinabol): Ishii et al., pl. 20, fig. 1.

2011 *Obeliscoites perspicuus* (Squinabol): Zyabrev et al., pl. 2, fig. 14.

Remarks: Test becomes asymmetrical from the second or third post-abdominal chambers.

Range: upper Barremian – upper Cenomanian (O'Dogherty, 1994).

Occurrence: Cosmopolitan.

Family Pseudodictyomitridae Pessagno, 1977b

Genus *Pseudodictyomitra* Pessagno, 1977b

Type species: *Pseudodictyomitra pentacolaensis* Pessagno, 1977b

Pseudodictyomitra lodogaensis Pessagno, 1977b

Figs 7.10-11, 13-14

1977b *Pseudodictyomitra lodogaensis* n. sp.: Pessagno, p. 50, pl. 8, figs. 4, 21, 28.

1992 *Pseudodictyomitra lodogaensis* n. sp.: Vishnevskaya, pl. 2, fig. 6.

1994 *Pseudodictyomitra lodogaensis* Pessagno: O'Dogherty, p.103, pl. 7, figs. 18-21. (cum syn.)

2001 *Pseudodictyomitra lodogaensis* Pessagno: Vishnevskaya, pl. 23, figs. 9, 10; pl. 86, fig. 11; pl. 123, figs. 26-28.

2008 *Pseudodictyomitra lodogaensis* Pessagno: Zyabrev et al., figs. 5. 25-26.

2011 *Pseudodictyomitra lodogaensis* Pessagno: Kurilov and Vishnevskaya, pl. 5, fig. 11.

2013 *Pseudodictyomitra lodogaensis* Pessagno: Zyabrev and Anoikin, pl., fig. 28.

2015 *Pseudodictyomitra lodogaensis* Pessagno: Zyabrev et al., fig. 4. 5.

Remarks: However the preservation is rather moderate or poor, the double rings of pores in strictures are visible, therefore we assign the specimens to *P. lodogaensis* Pessagno, 1977b.

Range: lower Aptian – Cenomanian (O'Dogherty, 1994).

Occurrence: Cosmopolitan.

Pseudodictyomitra sp. cf. *P. lodogaensis* Pessagno, 1977b

Figs 7.15-16

cf. 1977b *Pseudodictyomitra lodogaensis* n. sp.: Pessagno, p. 50, pl. 8, figs. 4, 21, 28.

Remarks: Only the first ring of pores (between thorax and abdomen) is single, all other rings of pores between post-abdominal chambers are double. Chambers contain massive, short costae. The rings of double pores are wider than at the holotype of *P. pentacolaensis* Pessagno.

Occurrence: Cosmopolitan.

Family Xitidae Pessagno, 1977b

Genus *Xitus* Pessagno, 1977b

Type species: *Xitus plenus* Pessagno, 1977b

Xitus mclaughlini (Pessagno, 1977b)

Figs. 8.1-2

1977b *Novixitus mclaughlini* n. sp.: Pessagno, p. 54, pl. 9, fig. 17.

1977b *Novixitus* sp. B.: Pessagno, p. 54, pl. 9, fig. 14.

1994 *Xitus mclaughlini* (Pessagno): O'Dogherty, p. 130, pl. 12, figs. 14-21. (cum syn.)

2011 *Xitus mclaughlini* (Pessagno): Zyabrev, pl. 3, fig. 37.

Remarks: This specimen is characterized by very large tubercles that arranged parallel rows. The illustrated specimen herein differs from holotype by the slightly smaller size of tubercles, only.

Range: upper Barremian – middle Cenomanian (O'Dogherty, 1994).

Occurrence: Cosmopolitan.

Xitus spinosus (Squinabol, 1904)

Fig. 8.3

1904 *Theocorys spinosa* n. sp.: Squinabol, p. 222, pl. 8, fig. 9.

1994 *Xitus spinosus* (Squinabol): O'Dogherty, p. 129, pl. 12, figs. 1-13. (cum syn.)

Remarks: The illustrated specimen has a small, asymmetrical apical horn with relatively large pores around the distal part of the spine. The outer latticed layer is slightly eroded.

Range: lower Albian – middle Cenomanian (O'Dogherty, 1994).

Occurrence: Cosmopolitan.

Xitus subitus Vishnevskaya, 1991

Fig. 8.7

1991 *Xitus subitus* n. sp.: Vishnevskaya, p. 93, pl. 2, figs. 3-4.

1992 *Xitus subitus* n. sp.: Vishnevskaya, p. 37, pl. 2, fig. 5.

2001 *Xitus subitus* Vishnevskaya: Vishnevskaya, p. 197, pl. 23, fig. 6; pl. 132, fig. 3-5.

2010 *Xitus subitus* Vishnevskaya: Palechek, pl. 3, fig. 4.

Range: Albian – Turonian.

Occurrence: Cuba, Eastern Kamchatka, USSR and Neh accretionary complex, Iran.

Xitus sp. cf. *X. spineus* Pessagno, 1977b

Fig. 8.4

Remarks: Due to poor preservation, this form cannot assign obviously to *X. spineus* Pessagno, 1977. It differs from *X. spineous* by more slender test and uniformly arranged double pores between chambers. Tubercles probably abraded, although they preserved at post-abdominal chambers.

Occurrence: Neh accretionary complex, Iran.

Xitus sp.

679 Figs. 8.8
680
681 Remarks: Due to missing apical part, this form can assign to the genus *Xitus.*
682 Occurrence: Neh accretionary complex, Iran.
683
684 Family: Xitomitridae O'Dogherty et al., 2017
685 Genus *Parvimitrella* O'Dogherty et al., 2017
686 Type species: *Pseudodictyomitrella wallacheri* Grill and Kozur, 1986
687
688 *Parvimitrella communis* (Squinabol, 1903)
689 Figs. 8.5-6
690
691 1903 *Stichomitra communis* n. sp.: Squinabol, p. 141, pl. 8, fig. 40.
692 1991 *Stichomitra communis* Squinabol: Basov and Vishnevskaya, p. 171, pl. 12, fig. 12; pl. 13, fig. 13; pl. 15,
693 figs. 6-9.
694 1992 *Stichomitra communis* Squinabol: Vishnevskaya, pl. 2, fig. 11.
695 1994 *Stichomitra communis* Squinabol: O'Dogherty, p. 144, pl. 17, figs. 6-16. (cum syn.)
696 2001 *Stichomitra communis* Squinabol: Vishnevskaya, pl. 23, fig. 8; pl. 79, fig. 3; pl. 129, fig. 8.
697 2004b *Stichomitra communis* Squinabol: Babazedah and De Wever, pl. 1, figs. 21-22.
698 2004 *Stichomitra communis* Squinabol: Bragina, p. 374, pl. 9, figs. 2, 6; pl. 32, figs. 10-12; pl. 33, fig. 16
699 2005 *Stichomitra communis* Squinabol: Vishnevskaya et al., pl. 2, fig. 26.
700 2007 *Stichomitra communis* Squinabol: Musavu-Moussavou et al., p. 271, pl. 4, figs. 7-8. (cum syn.)
701 2008 *Stichomitra communis* Squinabol: Baumgartner et al., pl. 5, fig. 13.
702 2008 *Stichomitra communis* Squinabol: Zyabrev et al., fig. 6. 41.
703 2010 *Stichomitra communis* Squinabol: Palechek et al., pl. 1, fig. 8, pl. 4, fig. 4, pl. 7, fig. 4.
704 2011 *Stichomitra communis* Squinabol: Zyabrev, pl. 3, fig. 11.
705 2012 *Stichomitra communis* Squinabol: Asis and Jasin, pl. 2, fig. 2.
706 2012 *Stichomitra stocki* (Cambell and Clark): Asis and Jasin, pl. 2, fig. 4.
707 2013 *Stichomitra communis* Squinabol: Zyabrev and Anoikin, pl. fig. 34.
708 2015 *Stichomitra communis* Squinabol: Shirdashtzadeh et al., figs. 3. 3-6.
709 2015 *Stichomitra communis* Squinabol: Zyabrev et al., fig. 4. 10.
710 2018 *Stichomitra communis* Squinabol: Kentri et al., figs. 8F-H. (cum syn.)
711 2019 *Parvimitrella communis* (Squinabol): Pirnia et al., figs. 3.7-8.
712
713 Remarks: The illustrated specimens herein possess conical, poreless cephalis. Thorax, abdomen and post-
714 abdominal chambers separated by relatively deep strictures. Thick wall with regularly distributed, large
715 hexagonal to polygonal pores.
716 Range: lower Aptian (O'Dogherty, 1994) – Coniacian-Santonian (Baumgartner et al., 2008).
717 Occurrence: Cosmopolitan.
718

Parvimitrella magna (Squinabol, 1904)

Fig. 8.10

1904 *Stichomitra magna* n. sp.: Squinabol, p. 234, pl. 10, fig. 8.

1994 *Stichomitra magna* Squinabol: O'Dogherty, p. 146, pl. 17, figs. 17-21. (cum syn.)

2004 *Stichomitra magna* Squinabol: Bragina, p. 375, Pl. 32, fig. 13.

Remarks: The preservation of this specimen is rather bad, however, I assigned to the *S. magna* Squinabol, because of the long, multi-segmented test with relatively large hexagonal to polygonal pores.

Range: middle Albian – middle Cenomanian (O'Dogherty, 1994).

Occurrence: Cosmopolitan.

Parvimitrella sp.

Fig. 8.9

Remarks: Cephalis absent in the illustrated specimen, thorax and abdomen spherical or slightly compressed. Post-abdominal chambers inflated (second post-abdominal chamber four times the size of the first post-abdominal chamber. Thick-walled test, having large pentagonal to polygonal pores at the thorax, abdomen and first post-abdominal chambers, while the second post-abdominal chamber possesses tetragonal pores in regular distribution.

Occurrence: Neh accretionary complex, Iran.

Family Arcanicapsinae Takemura, 1986

Genus *Dorypyle* Squinabol, 1904

Type species: *Dorypyle cretacea* Squinabol, 1904

Dorypyle communis (Squinabol, 1903)

Figs. 8.11-12

1903 *Xyphostylus communis* n. sp.: Squinabol, p. 111, pl. 10, fig. 20.

1994 *Dorypyle communis* (Squinabol): O'Dogherty, p. 204, pl. 32, figs. 11-19. (cum syn.)

2004a *Dorypyle communis* (Squinabol): Babazadeh and De Wever, p. 201, Figs 7W-X.

2011 *Dorypyle communis* (Squinabol): Zyabrev, pl. 1, fig. 33.

2015 *Dorypyle communis* (Squinabol): Zyabrev et al., fig. 4.15.

Range: middle – upper Albian (O'Dogherty, 1994).

Occurrence: Cosmopolitan.

Genus *Squinabollum* Dumitrica, 1970

Type species: *Clistophaena fossilis* Squinabol, 1903

Squinabollum fossile (Squinabol, 1903)

Figs. 8.13-14

1903 *Clistosphaera fossilis* n. sp.: Squinabol, p. 130, pl.10, fig. 11

1970 *Squinabollum fossilis* (Squinabol): Dumitrica, p. 83, pl.19, figs. 118a–118c, 119a–119c.

1992 *Squinabollum fossilis* (Squinabol): Vishnevskaya, pl. 2, fig. 14.

1994 *Squinabollum fossile* (Squinabol): O'Dogherty, p. 203, pl. 32, figs. 4–10. (cum syn.)

2001 *Squinabollum fossilis* (Squinabol): Vishnevskaya, pl. 22, figs. 6-11.

2007 *Squinabollum fossile* (Squinabol): Bragina et al., p. 318, pl. 2, fig. 13.

2011 *Squinabollum fossile* (Squinabol): Zyabrev, pl. 3, fig. 9.

2016 *Squinabollum fossile* (Squinabol): Bragina and Bragin, p. 25, Pl. 7, fig. 10. (cum syn.)

Remarks: Specimen in Fig. 8.14 differs from *S. fossile* (Squinabol, 1903) by lacking well-developed spines on the abdomen, they are probably broken away.

Range: Albian – Cenomanian-Santonian (Bragina and Bragin, 2006).

Occurrence: Neotethys.

Family Minocapsidae O'Dogherty et al., 2017

Crococapsa asseni (Tan, 1927)

Figs. 8.15-16

1927 *Cyrtocapsa Asseni* n. sp.: Tan, p. 67, pl. 14, fig. 118.

1994 *Hiscocapsa asseni* (Tan): O'Dogherty, p. 200, pl. 31, figs. 7-13. (cum syn.)

2003 *Hiscocapsa asseni* (Tan): Ziabrev et al., fig. 3.23.

2008 *Hiscocapsa asseni* (Tan): Zyabrev et al., fig. 6.23.

2011 *Hiscocapsa asseni* (Tan): Bandini et al., pl. 2, figs. 3-4.

2011 *Hiscocapsa asseni* (Tan): Zyabrev, pl. 2, fig. 5.

2011 *Hiscocapsa asseni* (Tan): Kurilov and Vishnevskaya, pl. 6, fig. 9.

2015 *Hiscocapsa asseni* (Tan): Shirdashtzadeh et al., figs. 5.5-6.

2019 *Crococapsa asseni* (Tan): Pirnia et al., fig. 3.4-5.

Range: upper Barremian – middle Albian (O'Dogherty, 1994).

Occurrence: Cosmopolitan

Crococapsa sp.

Fig. 8.18

Remarks: *Hiscocapsa* sp. is distinguished by possessing significantly higher cephalis without the apical horn. Thorax and abdomen are subcylindrical and well-developed, relatively large circular pores visible between them. Inflated post-abdominal chamber with large hexagonal to polygonal pores.

Occurrence: Neh accretionary complex, Iran.

Genus *Hiscocapsa* O'Dogherty, 1994

Type species: *Cyrtocapsa grutterinki* Tan, 1927

Hiscocapsa grutterinki (Tan, 1927)

Fig. 8.17

1927 *Cyrtocapsa Grutterinki* n. sp.: Tan, p. 64, pl. 13, fig. 110.

1994 *Hiscocapsa grutterinki* (Tan): O'Dogherty, p. 201, pl. 31, figs. 14-16; pl. 32, figs. 1-3. (cum syn.)

1994 *Cyrtocapsa* (?) *grutterinki* Tan: Jud, p. 74, pl. 8, fig. 12; pl. 9, fig. 1.

2003 *Hiscocapsa grutterinki* (Tan): Zyabrev et al., figs. 3.24.

2011 *Hiscocapsa grutterinki* (Tan): Kurilov and Vishnevskaya, pl. 6, fig. 8.

2013 *Hiscocapsa grutterinki* (Tan): Zyabrev and Anoikin, pl., fig. 18.

Remarks: On the surface of the test many tubercles are visible, on the basis of this it can be easily distinguished from other species of *Hiscocapsa*.

Range: Barremian – pper Aptian.

Occurrence: Cosmopolitan

5. Discussion

The Sistan suture zone (SSZ) in Eastern Iran plays a critical role in the geodynamic reconstruction of the Neotethyan suture zone. The polarity of the Neh accretionary prism and Sefidabeh forearc basin, and the general younging of the accretionary prisms to the southwest as well as some other geological evidence have been used to postulate a northeast-dipping subduction under the Afghan block. According to this model, one would expect to find the youngest parts of accretionary prisms adjacent to the Lut block. However, our new radiolarian age from the Dumak area contradicts this model. In this region the oceanic lithosphere is commonly intercalated with massive radiolarian chert, therefore stratigraphic dating of this radiolarite provides age constraints for time of oceanic lithosphere formation. Only two radiolarian biostratigraphic studies from the SSZ from eastern Iran have been published so far (Babazadeh and De Wever, 2004a, b), reporting two rather moderately preserved and moderately diverse radiolarian assemblages from Soulabest village. Those assemblages were obtained from red argillaceous cherts and green-grey cherts from the Ratuk ophiolite complex and were considered early Aptian and middle-late Albian in age (Babazadeh and De Wever, 2004a). Our sample examined herein contains a relatively well to moderately preserved and diverse radiolarian fauna, with an assemblage of 19 spumellarian and 26 nassellarian species. The biostratigraphically most important species are short-ranging (dominantly Albian or Albian to Cenomanian) forms such as *Dactyliodiscus cayeuxi* Squinabol, 1903, *Thanarla brouweri* (Tan, 1927),

Dictyomitra obesa (Squinabol, 1903), *Xitus spinosus* (Squinabol, 1904), *Parvimitrella magna* Squinabol, 1904 and *Dorypyle communis* (Squinabol, 1903). This assemblage is assigned to the middle Albian – lower Cenomanian Spoletoensis radiolarian zone including the Romanus and Missilis radiolarian subzones, that allows correlation with UA 10–13 of O'Dogherty (1994), but a more precise biostratigraphic range suggests a middle Albian age (Romanus and most likely Missilis subzone by O'Dogherty, 1994). This radiolarian fauna suggests that sampled radiolarite was deposited during the mid-Cretaceous which also determines the time of oceanic crust formation. This radiolarian fauna from the Dumak ophiolitic mélange contains a typical mid-Cretaceous radiolarian assemblage that compares well with that published in the outstanding monograph of O'Dogherty (1994), although quite similar radiolarian faunas have been also reported from Iran (Pessagno et al., 2005, Babazadeh, 2007, Babazadeh and De Wever, 2004a, Gharib and De Wever, 2010, Shirdashtzadeh et al., 2015 and Pirnia et al., 2019), Crimea (Kopaevich, Vishnevskaya, 2016), southern Tibet (Ziabrev et al., 2003), India (Bragina and Bragin, 2013), Eastern Russia (Zyabrev, 1996; 2011; Kurilov and Vishnevskaya, 2011), Malaysia (Jasin, 1992; 2018; Asis and Jasin, 2012; Jasin and Tongkul, 2012), Indonesia (Jasin and Haile, 1996), as well as from Cuba (Vishnevskaya, 2001).

6. Conclusions

A relatively well-preserved and diverse radiolarian fauna from the Dumak ophiolitic mélange of the Sistan suture zone in Eastern Iran is reported herein. The radiolarian fauna was obtained from a deep marine sedimentary succession associated with basalts. The radiolarite succession represents pelagic strata deposited near an oceanic spreading center. The radiolarian fauna suggests a middle to late Albian age which also determines the time of oceanic crust formation.

Acknowledgments

The authors are thankful to Dr. Špela Goričan, SAZU, Ljubljana and one anonymous reviewer for their suggestions and critical comments. The helpful comments of journal editor Dr. Eduardo Koutsoukos were greatly appreciated. We thank Prof. József Pálfy (Budapest) for improving the English text. This work was supported by the Iran National Science Foundation (97011420). The present study is MTA-MTM-ELTE paleo contribution No. 297.

References

Agard, P., Jolivet, L., Vrielynck, B., Burov, E., Monié, P., 2007. Plate acceleration: the obduction trigger? Earth and Planetary Science Letters 258, 428-441.

Agard, P., Omrani, J., Jolivet, L., Whitechurch, H., Vrielynck, B., Spakman, W., Monie, P., Meyer, B., Wortel, R., 2011. Zagros orogeny: a subduction-dominated process. Geological Magazine 148, 692-725.

Aliev, K. S., 1965. Radiolarians of the Lower Cretaceous deposits of northeastern Azerbaidzhan and their stratigraphic significance, Izdatel'stvo Akademii Nauk, Azerbaidzhanskoi SSR, Baku, 1-124.

Arjmandzadeh, R., Karimpour, M., Mazaheri, S., Santos, J., Medina, J., Homam, S., 2010. Two sided asymmetric subduction: new hypothesis for the tectonomoagmatic and metallogenic setting of the Lut Block, Eastern Iran. Journal of Economic Geology 3(1), 17-30.

Asis, J., Jasin, B., 2012. Aptian to Turonian Radiolaria from the Darvel Bay Ophiolite Complex, Kunak, Sabah. Bulletin of the Geological Society of Malaysia 58, 89-96.

Babazadeh, S. A., 2007. Cretaceous radiolarians from Birjand ophiolitic range in Sahlabad province, eastern Iran. Revue de Paléobiologie 26(1), 89-98.

Babazadeh, S. A., De Wever, P., 2004a. Early Cretaceous radiolarian assemblages from radiolarites in the Sistan Suture (eastern Iran). Geodiversitas 26(2), 185-206.

Babazadeh, S. A., De Wever, P., 2004b. Radiolarian Cretaceous age of Soulabest radiolarites in ophiolite suite of eastern Iran. Bulletin de la Société Géologique de France 175(2), 121-129.

Bandini, A. N., Baumgartner, P. O., Flores, K., Dumitrica, P., Hochard, C., Stampfli, G., Jackett, S.J., 2011. Aalenian to Cenomanian Radiolaria of the Bermeja Complex (Puerto Rico) and Pacific origin of radiolarites on the Caribbean Plate. Swiss Journal of Geosciences 104(3), 367-408.

Basov I.A., Vishnevskaya V.S., 1991. Upper Mesozoic Stratigraphy of the Pacific Ocean. Nauka, Moscow, 1–200.

Baumgartner, P.O., 1980. Late Jurassic Hagiastridae and Patulibracchiidae (Radiolaria) from the Argolis Peninsula (Peloponnesus, Greece). Micropaleontology 26, 274-322.

Baumgartner, P. O., Flores, K., Bandini, A. N., Girault, F., Cruz, D., 2008. Upper Triassic to Cretaceous radiolaria from Nicaragua and Northern Costa Rica - The Mesquito Composite Oceanic Terrane. Ofioliti 33(1), 1-19.

Baumgartner, P.O., O'Dogherty, L., Goričan, Š.,., Urquhart, E., Pillevuit, A., De Wever, P., 1995. Middle Jurassic to Lower Cretaceous Radiolaria of Tethys: Occurrences, Systematics, Biochronology. Mémoires de Géologie (Lausanne) 23, 1-1172.

Bortolotti, V., Principi, G., 2005. Tethyan ophiolites and Pangea break-up. Island Arc 14, 442-470.

Bragina, L.G., 2004. Cenomanian-Turonian radiolarians of northern Turkey and the Crimean Mountains. Paleontological Journal 38, 325-456.

Bragina, L. G., 2009. Radiolarians and stratigraphy of Cenomanian-Coniacian deposits in the Crimean and West Sakhalin Mountains, Pt. 2: Comparative analysis. Stratigraphy and Geological Correlation 17(4), 430-442.

Bragina, L. G., Agarkov, Y. V., Bragin, N. Y., 2007, Radiolarians of the Upper Cenomanian and Lower Turonian from Deposits of the Ananuri Formation, the Western Caucasus (Lazarevskoe Area). Stratigraphy and Geological Correlation 15(3), 310-320.

Bragina, L. G., Bragin, N. Y., 2004. Radiolarians from Upper Cretaceous Deposits, the Novodeviche Section (Samara Oblast, Volga River Middle Courses). Stratigraphy and Geological Correlation 12(3), 286-296.

Bragina, L. G., Bragin, N. Y., 2006, Stratigraphy and Radiolarians of Upper Cretaceous Sedimentary Cover of the Arakapas Ophiolite Massif (Cyprus): Stratigraphy and Geological Correlation 14(5), 507-523.

Bragina, L. G., Bragin, N., 2013. New data on the Albian-Cenomanian radiolarians from the Karai Formation (South India). Stratigraphy and Geological Correlation 21(5), 515-530.

Bragina, L. G., Bragin, N., 2015. New Data on Albian–Coniacian Radiolarians from the Kelevudag Section (Northeastern Azerbaijan). Stratigraphy and Geological Correlation 23(1), 45-56.

Bragina, L. G., Bragin, N., 2016. Cretaceous (Albian to Turonian) radiolarians from chert blocks of the Moni Mélange (Southern Cyprus). Revue de Micropaléontologie 59(4), 311-338.

Bröcker, M., Fotoohi Rad, G.R., Theunissen, S., 2010. New time constraints for HP metamorphism and exhumation of mélange rocks from the Sistan suture zone, Eastern Iran. Tectonic Crossroads: Evolving Orogens of Eurasia-Africa-Arabia. Session No. 13. Ophiolites, blueschists, and suture zones.

Bröcker, M., Fotoohi Rad, G.R., Burgess, R., Theunissen, S., Paderin, I., Rodionov, N., Salimi, Z., 2013. New age constraints for the geodynamic evolution of the Sistan Suture Zone, eastern Iran. Lithos 170–171, 17-34.

Camp, V.E, Griffis, R.J., 1982. Character, Genesis and Tectonic Setting of Igneous Rocks in the Sistan suture zone, Eastern Iran. Lithos 15, 221-239.

Danelian, T., 2008. Diversity and biotic changes of Archaeodictyomitrid Radiolaria from the Aptian/Albian transition (OAE1b) of southern Albania. Micropaleontology 54, 3-13.

Danelian, T., Baudin, F., Gardin, S., Masure, E., Ricordel, C., Fili, I., Mecaj, T., Muska, K., 2007. The record of mid Cretaceous oceanic anoxic events from the Ionian zone of southern Albania. Revue de Micropaléontologie 50, 225-237.

Deflandre, G., 1953. Radiolaires fossiles, in: Grassé, P.P. (Ed.), Traité de Zoologie. Masson, Paris, 389-436.

Delaloye, M., Desmons, J., 1980. Ophiolites and mélange terranes in Iran: a geochronological study and ITS paleotectonic implications. Tectonophysics 68(1-2), 83-111.

Delavari, M., Amini, S., Saccani, E., and Beccaluva, L., 2009. Geochemistry and Petrogenesis of Mantle Peridotites from the Nehbandan Ophiolitic Complex, Eastern Iran. Journal of Applied Science 9, 2671-2687.

Dilek, Y., Furnes, H., Shallo, M., 2007. Suprasubduction zone ophiolite formation along the periphery of Mesozoic Gondwana. Gondwana Research 11, 453-475.

Donofrio, D., Mostler, H, 1978. Zur Verbreitung der Saturnalidae (Radiolaria) im Mesozoikum der Nördlichen Kalkalpan und Südalpen. Geologisch Paläontologische Mitteilungen Innsbruck 7, 1-55.

Dumitrica, P., 1970. Cryptocephalic and cryptothoracic Nassellaria in some Mesozoic deposits of Romania. Revue Roumaine de Géologie, Géophysique et Géographie (série Géologie) 14, 45-124.

Dumitrica, P., Immenhauser, A., Dumitrica-Jud, R., 1997. Mesozoic Radiolarian Biostratigraphy from Masirah Ophiolite, Sultanate of Oman Part I: Middle Triassic, Uppermost Jurassic and Lower Cretaceous Spumellarians and Multisegmented Nassellarians. Bulletin of the National Museum of Natural Science, Taiwan 9, 1-106.

Ehrenberg, C. G., 1838, Über die Bildung der Kreidefelsen und des Kreidemergels durch unsichtbare Organismen: Abhandlungen der Königlich Preussischen Akademie der Wissenschaften zu Berlin, 59-147.

Ehrenberg, C. G., 1875, Fortsetzung der mikrogeologischen Studien als Gesammt-Uebersichtder mikroskopischen Paläontologie gleichartig analysirter Gebirgsarten der Erde, mit specieller Rücksicht auf den Polycystinen-Mergel von Barbados: Abhandlungen der Königlich Preussischen Akademie der Wissenschaften zu Berlin, 1-225.

Erbacher, J., Thurow, J., 1997. Influence of Oceanic Anoxic Events on the evolution of mid-Cretaceous Radiolaria in the North Atlantic and Western Tethys. Marine Micropaleontology 30, 139-158.

Foreman, H.P., 1973. Radiolaria from DSDP Leg 20. In: Heezen, B. C. et. al. (Eds), Initial Reports of the Deep Sea Drilling Project. U.S. Government Printing Office, Washington, D.C, 249-305.

Foreman, H.P., 1975. Radiolaria from the North Pacific, Deep Sea Drilling Project, Leg 32. In: Larson, R.L.et al. (Eds), Initial Reports of the Deep Sea Drilling Project. U.S. Government Printing Office, Washington, D.C, 579-676.

Fotoohi Rad, G.R., Droop, G.T.R., Amini, S., Moazzen, M., 2005. Eclogites and blueschists of the Sistan Suture Zone, eastern Iran: a comparison of P-T histories from a subduction melange. Lithos 84(1-2), 1-24.

Gharib, F., De Wever, P., 2010. Mesozoic radiolarians from the Kermanshah formation (Iran). Comptes Rendus Palevol 9, 209-219.

Górka, H., 1989. Les Radiolaires du Campanien inférieur de Cracovie (Pologne). Acta Palaeontologica Polonica 34(4), 327-354.

Grill, J., Kozur, H., 1986. The first evidence of the *Unuma echinatus* radiolarian zone in the Rudabanya Mts. (northern Hungary). Geologisch Paläontologische Mitteilungen Innsbruck 13, 239-275.

Haeckel, E., 1862. Die Radiolarien (Rhizopoda Radiaria). Eine Monographie. Reimer, Berlin.

Haeckel, E., 1881. Entwurf eines Radiolarien-Systems auf Grund von Studien der Challenger-Radiolarien. Jenaische Zeitschrift für Naturwissenschaft 15, 418-472.

Hori, N., 1999. Latest Jurassic radiolarians from the northeastern part of the Torinoko Block, Yamizo Mountains, central Japan. Science Reports of the Institute of Geoscience, University of Tsukuba, Section B: Geological Sciences 20, 47-114.

Hull, D.M., 1997. Upper Jurassic Tethyan and southern boreal radiolarians from western North America. Micropaleontology 43, 1-202.

Ishii, Y., Suzuki, N., Kano, H., 2009. Berriasian-Barremian (Early Cretaceous) radiolarians from paleo-Pacific regions (DSDP and ODP Holes 463, 800A, 801B, 765C, 1213B, and the Goshikigahama bedded red shale of the Nothern Shimant Belt. News of Osaka Micropaleontologists 14, 317-373.

Jasin, B., 1992. Significance of radiolarian cherts from the Chert-Spilite Formation, Telupid, Sabah. Bulletin of the Geological Society of Malaysia 31, 67-83.

Jasin, B., 2000. Geological significance of radiolarian chert in Sabah. Geol. Soc. Malaysia Bulletin 44, 33-43.

Jasin, B., 2018. Radiolarian biostratigraphy of Malaysia. Bulletin of the Geological Society of Malaysia 65, 45-58.

Jasin, B., Tongkul, F., 2012. Cretaceous radiolarians from Baliojong ophiolite sequence, Sabah, Malaysia. Journal of Asian Earth Sciences 76, 258-265.

Jasin, B., Haile, N., 1996. Uppermost Jurassic Lower Cretaceous Radiolarian chert from the Tanimbar Islands (Banda Arc), Indonesia. Journal of Southeast Asian Earth Sciences 14(1-2), 91-100.

Jud, R., 1994. Biochronology and systematics of Early Cretaceous Radiolarian of the Western Tethys. Mémoires de Géologie (Lausanne) 19, 1-147.

Kentri, T., Fadhel, M., Benyoucef, M., Adaci, M., Piuz, A., Bensalah, M., Mahboubi, M., Gallala, N. 2018. The Cenomanian–Turonian transition in Northwestern Algeria (Douar Menkouchi Section, Ouarsenis): Radiolarian biostratigraphy. Annales de Paléontologie 104(2), 81-99.

Kiessling, W., 1995. Palökologische Verwertbarkeit oberjurassisch-unterkretazischer Radiolarienfaunen mit Beispielen aus Antarktis, Oman und Südalpen. In: Paleoecological use of Late Jurassic-Early Cretaceous radiolarians with examples from the Southern Alps, O.M.a.A.P. (Ed.), Geowissenschaftlichen Fakultät. Friedrich-Alexander-Universität (Unpublished), Erlangen-Nürnberg. 465 pp.

Kopaevich L., Vishnevskaya V., 2016. Cenomanian–Campanian (Late Cretaceous) planktonic assemblages of the Crimea–Caucasus area: Palaeoceanography, palaeoclimate and sea level changes. Palaeogeography, Palaeoclimatology, Palaeoecology 441, 493-515.

Kozur, H., Mostler, H., 1981. Beiträge zur Erforschung der mesozoischen Radiolarien. Teil IV: Thalassosphaeracea HAECKEL, 1862, Hexastylacea HAECKEL, 1862 emend. PETRUŠEVSKAJA, 1979, Sponguracea HAECKEL, 1862 emend. und weitere triassische Lithocycliacea, Trematodiscacea, Actinommacea und Nassellaria. Geologisch Paläontologische Mitteilungen Innsbruck, Sonderband 1, 1-208.

Kozur, H., Mostler, H., 1994. Anisian to middle Carnian radiolarian zonation and description of some stratigraphically important radiolarians. Geologisch Paläontologische Mitteilungen Innsbruck, Sonderband 3, 39-255.

Kurilov D. V., Vishnevskaya V. S. 2011. Early Cretaceous Radiolarian Assemblages from the East Sakhalin Mountains. Stratigraphy and Geological Correlation 19(1), 44-62.

Kurogi, Y., Takahashi, O., 2009, Shortening of thrust zones and role of the Butsuzo Tectonic Line as an out-of-sequence thrust in Mesozoic accretionary complexes of Ume-machi, Oita Prefecture, Southwest Japan: News of Osaka Micropaleontologists 14, 405-412.

Lahm, B., 1984. Spumellarienfaunen (Radiolaria) aus den mitteltriassischen Buchensteiner-Schichten von Recoaro (Norditalien) und den obertriassischen Reiflingerkalken von Grosreifling (Österreich). Systematik, Stratigraphie. Münchner geowissenschaftliche Abhandlungen. Reihe A, Geologie und Paläontologie 1, 1-161.

Matsuoka, A., 1998. Faunal composition of earliest Cretaceous (Berriasian) radiolaria from the Mariana Trench in the western Pacific. News of Osaka Micropaleontologists, special volume 11, 165-187.

Maurizot, P., 1979. Geology of the Gazik quadrangle, 1:250000 scale. Report submitted to the Geological and Mineral Survey of Iran, 1-172.

McCall, G. J.H., 1997. The geotectonic history of the Makran and adjacent area of southern Iran. Journal of Asian Earth Sciences 15, 517-531.

McCall, G.J.H., 2002. A summary of the geology of the Iranian Makran. Geol. Soc. London, Spec. Publ. 195, 147–204.

Musavu-Moussavou, B., Danelian, T., 2006. The Radiolarian biotic response to Oceanic Anoxic Event 2 in the southern part of the Northern proto-Atlantic (Demerara Rise, ODP Leg 207). Revue de Micropaléontologie 49(3), 141-163.

Musavu-Moussavou, B., Danelian, T., Baudin, F., Coccioni, R., Fröhlich, F., 2007. The Radiolarian biotic response during OAE2. A high-resolution study across the Bonarelli level at Bottaccione (Gubbio, Italy). Revue de Micropaléontologie 50, 253-287.

Müller, J., 1858, Über die Thalassicollen, Polycystinen und Acanthometren des Mittelmeeres. Abhandlungen der Königlich Preussischen Akademie der Wissenschaften zu Berlin, 1-62.

O'Dogherty, L., 1994. Biochronology and Paleontology of Mid-Cretaceous Radiolarians from Northern Apennines (Italy) and Betic Cordillera (Spain). Mémoires de Géologie (Lausanne) 21, 1-415.

O'Dogherty, L., Goričan, Š., Gawlick, H.J., 2017. Middle and Late Jurassic radiolarians from the Neotethys suture in the Eastern Alps. Journal of Paleontology 91, 25-72.

Ogg, J. G., Ogg, G. M., Gradstein F. M., 2016. Cretaceous. In: Ogg, J. G, Ogg, G. M., Gradstein F. M., (Eds.), A Concise Geologic Time Scale. Elsevier B. V., 167-186.

Ozsvárt, P., Moix, P., Kozur, H., 2015. New Carnian (Upper Triassic) radiolarians from the Sorgun Ophiolitic Mélange, Southern Turkey. Neues Jahrbuch für Geologie und Paläontologie Abhandlungen 277(3), 337-352.

Ozvoldová, L., 1979. Radiolarians from Rudina beds of the Kysuca series in the Klippen belt from locality Brodno. Annotationes Zoologicae et Botanicae 128, 1-15.

Palechek, T., Savel'ev, D., Savel'eva, O., 2010, Albian-Cenomanian Radiolarian Assemblage from the Smaginsk Formation, the Kamchatskii Mys Peninsula of Eastern Kamchatka. Stratigraphy and Geological Correlation 18(1), 63-82.

Pang, K.N., Chung, S.L., Zarrinkoub, M.H., Mohammadi, S.S., Yang, H.M., Chu, C.H., Lee, H.Y., Lo, C.H., 2012. Age, geochemical characteristics and petrogenesis of Late Cenozoic intraplate alkali basalts in the Lut–Sistan region, eastern Iran. Chemical Geology 306-307(4), 40-53.

Pantanelli, D., 1880. I diaspri della Toscana e i loro fossili. Atti della Reale Accademia nazionale dei Lincei, Memorie della Classe di Scienze fisiche, matematiche e naturali 8, 35-66.

Parona, C. F., 1890. Radiolarie nei noduli selciosi del calcare giurese di Cittiglio presso Laverno. Bollettino della Società Geologica Italiana 9, 132-175.

Pessagno, E.A., 1969. The Neosciadiocapsidae, a new family of Upper Cretaceous Radiolaria. Bulletins of American Paleontology 56, 377-439.

Pessagno, E. A., 1971. Jurassic and Cretaceous Hagiastridae from the Blake-Bahama Basin (Site 5A, JOIDES Leg 1) and the Great Valley Sequence, California Coast Ranges. Bulletins of American Paleontology 60, 5-83.

Pessagno, E. A., 1973. Upper Cretaceous Spumellariina from the Great Valley Sequence, California Coast Ranges. Bulletins of American Paleontology 63, 49-102.

Pessagno, E.A., 1976. Radiolarian zonation and stratigraphy of the Upper Cretaceous portion of the Great Valley Sequence, California Coast Ranges. Micropaleontology, Special Publication 2, 1-95.

Pessagno, E. A., 1977a, Upper Jurassic Radiolaria and radiolarian biostratigraphy of the California Coast Ranges. Micropaleontology 23(1), 56-113.

Pessagno, E. A., 1977b, Lower Cretaceous radiolarian biostratigraphy of the Great Valley Sequence and Franciscan Complex, California Coast Ranges. Cushman Foundation for foraminiferal Research 15, 1-87.

Pessagno, E. A. J., Ghazi, A. M., Kariminia, M., Duncan, R. A., and Hassanipak, A. A., 2005. Tectonostratigraphy of the Khoy Complex, northwestern Iran. Stratigraphy 2,49-63.

Pessagno, E. A., Newport, R. L., 1972. A technique for extracting Radiolaria from radiolarian cherts. Micropaleontology 18(2), 231-234.

Pessagno, E. A., Six, W. M., Yang, Q., 1989. The Xiphostylidae Haeckel and Parvivaccidae, n. fam., (Radiolaria) from the North American Jurassic. Micropaleontology 35(3) 193-255.

Pirnia, T., Saccani, E., Torabi, G., Chiari, M., Goričan, Š., Barbero, E., 2019. Cretaceous tectonic evolution of the Neo-Tethys in Central Iran: Evidence from petrology and age of the Nain-Ashin ophiolitic basalts. Geoscience Frontiers 11(1), 57-81.

Riedel, W. R., 1967. Subclass Radiolaria. in Harland, W. B., Holland, C. H., House, M. R., Hughes, N. F., Reynolds, A. B., Rudwick, M. J. S., Satterthwaite, G. E., Tarlo, L. B. H., Willey, E. C., (Eds.) The Fossil Record. Geological Society of London, 291-298.

Riedel, W. R., 1971. Systematic classification of polycystine Radiolaria. In: Funnell, B. M., Riedel, W. R., (Eds.), The Micropalaeontology of Oceans. Cambridge, UK, Cambridge University Press, 649-660.

Robertson, A.H.F., 2002. Overview of the genesis and emplacement of Mesozoic ophiolites in the Eastern Mediterranean Tethyan region. Lithos 65, 1-67.

Robertson, A. H. F., 2004. Development of Concepts Concerning the Genesis and Emplacement of Tethyan Ophiolites in the Eastern Mediterranean and Oman Regions. Earth-Science Reviews 66, 331-387.

Robin, C., Goričan, Š., Guillocheau, F., Razin, P., Dromart, G., Mosaffa, H., 2010. Mesozoic deep-water carbonate deposits from the southern Tethyan passive margin in Iran (Pichakun nappes, Neyriz area): biostratigraphy, facies sedimentology and sequence stratigraphy. In: Leturmy, P., Robin, C., (Eds.), Tectonic and Stratigraphic Evolution of Zagros and Makran during the Mesozoic–Cenozoic. Special Publications of the Geological Society of London 330, 179-210.

Rüst, D., 1898. Neue Beiträge zur Kenntniss der Fossilen Radiolarien aus Gesteinen des Jura und der Kreide. Palaeontographica 45, 1-67.

Saccani, E., Delavari, M., Beccaluva, L., Amini, S., 2010. Petrological and geochemical constraints on the origin of the Nehbandan ophiolitic complex (eastern Iran): implication for the evolution of the Sistan Ocean. Lithos 117, 209-228.

Salvini, G., Marcucci Passerini, M., 1998. The radiolarian assemblages of the Bonarelli Horizon in the Umbria-Marche Apennines and Southern Alps, Italy. Cretaceous Research 19, 777-804.

Schmid, S.M., Bernoulli, D., Fügenschuh, B., Matenco, L., Scheffer, S., Schuster, R., Tischler, M., Ustaszewski, K., 2008. The Alps-Carpathians-Dinarides-connection: a correlation of tectonic unit. Swiss Journal of Geosciences 101(1), 139-183.

Şengör, A.M.C., Yilmaz, Y., Sungurlu, O., 1984. Tectonics of the Mediterranean Cimmerides: nature and evolution of the western termination of PaleoTethys. In: Dixon, J.E., Robertson, A.H.F. (Eds.), The Geological Evolution of the Eastern Mediterranean. Geological Society of London Special Publication 17, 77-112.

Shirdashtzadeh, N., Kachovich, S., Aitchison, J., Samadi, R., 2015. Mid-Cretaceous radiolarian faunas from the Ashin Ophiolite (western Central-East Iranian Microcontinent). Cretaceous Research 56, 110-118.

Smrečková, M., 2011. Lower Turonian radiolarians from the Červená skala section (Pieniny Klippen Belt, Western Carpathians). Mineralia Slovaca 43, 31- 38.

Snoke, A.W., Noble, P.J., 2001. Ammonite-radiolarian assemblage, Tobago Volcanic Group, Tobago, West Indies - Implications for the evolution of the Great Arc of the Caribbean. Geological Society of America, Bulletin 113, 256-264.

Squinabol, S., 1903. Le Radiolarie dei noduli selciosi nella Scaglia degli Euganei. Contribuzione I. Rivista Italiana di Paleontologia 9, 105-151.

Squinabol, S., 1904. Radiolarie cretacee degli Euganei. Atti e Memorie della Reale Accademia di Scienze, Lettere ed Arti in Padova 20, 171-244.

Squinabol, S., 1914. Contributo alla conoscenza dei Radiolarii fossili del Veneto. Appendice - Di un genera di Radiolari caratteristico del Secondario. Memorie dell'Istituto Geologico della Reale Universita di Padova 2, 249-306.

Stampfli G.M., Kozur H.W., 2006. Europe from the Variscan to the Alpine cycles. In: Gee, D.G., Stephenson, R.A. (Eds.), European lithosphere dynamics. Geological Society of London Memoir 32, 43-56.

Stöcklin, J. 1977. Structural correlation of the Alpine ranges between Iran and Central Asia. Société Géologique de France, Mémoire 8, 333-353.

Takemura, A., 1986. Classification of Jurassic Nassellarians (Radiolaria). Palaeontographica. Abteilung A: Palaozoologie-Stratigraphie 195, 29-74.

Tan, S.H., 1927. Over de samenstelling en het onstaan van krijt- en mergel-gesteenten van de Molukken, Jaarboek van het mijnwezen in Nederlandsch Oost-Indie, jaargang 55 (1926), verhandelingen, 3rd gedeelte, pp. 5-165.

Thurow, J., 1988. Cretaceous radiolarians of the North Atlantic Ocean: ODP Leg 103 (Sites 638, 640 and 641) and DSDP Legs 93 (Site 603) and 47B (Site 398). In: Boillot, G., t al. (Eds.). Proceedings of the Ocean Drilling Program, Scientific Results. College Station, TX (Ocean Drilling Program), 379-418.

Tirrul, R., Bell, I.R., Griffis, R.J., Camp, V.E. 1983. The Sistan Suture Zone in Eastern Iran. Geological Society of America Bulletin 94, 134-150.

Urquhart, E., 1994, New Data on the Ranges of Some Cretaceous Tethyan Radiolaria: Comptes Rendus de l'Académie des Sciences de Paris, Série II, 318(2), 1401-1407.

Vishnevskaya, V. S., 1991. New representatives of Mesozoic radiolarians. In: Tochilina, S. V., (Ed.), Paleontological and stratigraphic investigation of Phanerozoic in the Far Eastern Region (by the results of radiolarian analysis for mapping). Academy of Science of the USSR Far Eastern Division. Pacific Oceanological Institute, 89-99.

Vishnevskaya, V. S., 1992. Significance of Mesozoic radiolarians for tectonostratigraphy in Pacific Rim terranes of the former USSR. Palaeogeography, Palaeoclimatology, Palaeoecology 96, 23-39.

Vishnevskaya, V. S., 2001. Jurassic to Cretaceous radiolarian biostratigraphy of Russia, Moscow, GEOS, 1-376.

Vishnevskaya, V. S., Kazintsova, L. I., Kopaevich, L. F., 2005. Radiolarians across the Albian-Cenomanian Boundary (Examples from the Russian Platform). Stratigraphy and Geological Correlation 13(4), 438-452.

Wu, H.R., 1986. Some new genera and species of Cenomanian Radiolaria from southern Xizang (Tibet). Acta Micropalaeontologica Sinica 3, 354-359.

Xu, B., Luo. H., 2017. Age of the radiolarian chert from the Zhilong section in Gyangze, southern Tibet and its implications. Palaeoworld 26, 159-172.

Yang, Q., 1993. Taxonomic Studies of Upper Jurassic (Tithonian) Radiolaria from the Taman Formation, east-central Mexico. Palaeoworld 3, 1-164.

Ziabrev, S., Aitchison, J., Abrajevitch, A., Badengzhu, Davis, A, Luo, H, 2003. Precise radiolarian age constraints on the timing of ophiolite generation and sedimentation in the Dazhuqu terrane, Yarlung–Tsangpo suture zone, Tibet. Journal of the Geological Society of London 160, 591-599.

Zittel, K.A., 1876. Über einige fossile Radiolarien aus der norddeutschen Kreiden. Zeitschrift der deutschen geologischen Gesellschaft 28, 75-87.

1267 Zyabrev, S. V., 1996. Cretaceous radiolarian fauna from the Kiselyovsky subterrane, the youngest accretionary
1268 complex of the Russian continental far east: Paleotectonic and paleogeographic implications. The Island Arc
1269 5(2), 140-155.
1270
1271 Zyabrev, S. V., 2011. Stratigraphy and structure of the central East Sakhalin accretionary wedge (Eastern
1272 Russia). Russian Journal of Pacific Geology 5, 313-335.
1273
1274 Zyabrev, S., Anoikin, V. I., 2013. New data on the ages of deposits in the Kiselevka-Manoma accretionary
1275 complex based on radiolarian fossils. Russian Journal of Pacific Geology 7(3), 217-225.
1276
1277 Zyabrev, S., Anoikin, V., Kudymov, V., 2015. Structure, Age, and Mechanism of Emplacement of the Amur and
1278 Kiselevka–Manoma Accretionary Complexes of the Lower Amur Region, Russian Far East. Geotectonics 49,
1279 65-79.
1280
1281 Zyabrev, S.V., Kojima, S., Ahmad, T., 2008. Radiolarian biostratigraphic constraints on the generation of the
1282 Nidar ophiolite and the onset of Dras are volcanism: Tracing the evolution of the closing Tethys along the Indus
1283 - Yarlung-Tsangpo suture. Stratigraphy 5, 99-112.

Figure captions

Figure 1 a) Generalised tectonic map of the Middle East, showing the location of the Sistan Suture Zone between the Afghan and Lut blocks (modified from Tirrul et al. 1983). (b) The Sistan suture zone of eastern Iran and its major subdivisions (modified from Tirrul et al. 1983).

Figure 2 Simplified geologic map of the Dumak ophiolitic melange with the location of the analyzed sample (Shu95-3) with Section of Dumak ophiolitic mélange with the position of the radiolarites studied in Shuru and simplified stratigraphical column of pelagic sediments overlying the Dumak ophiolite in the Shuru area.

Figure 3 The sequence of red radiolarites with basalt in the Shuru region. Shu-95 sample comes from the middle part of the red massive radiolarite outcrop.

Figure 4 Stratigraphic ranges of radiolarian taxaof sample Shu95-3, the Neh accretionary complex, Eastern Iran. Radiolarian Unitary Associations and biostratigraphic zonation based on O'Dogherty, 1994 and timescale calibrated after Ogg et al., 2016.

Figure 5 1. *Archaeocenosphaera clathrata* (Parona, 1890) (INV 2019.2768); 2. *Acaeniotyle diaphorogona* Foreman, 1973 (INV 2019.2769); 3-4. *Acaeniotyle umbilicata* (Rüst, 1898) (INV 2019.2770.1 and INV 2019.2770.2); 5. *Acaeniotyle* sp. cf. *A.* sp. A. Thurow, 1988 (INV 2019.2771); 6-8. *Tetrapaurinella* sp. 1. (INV 2019.2772.1,INV 2019.2772.2, INV.2019.2772.3); 9. *Tetrapaurinella* sp. cf. *T. staurus* Dumitrica, 1997 (INV 2019.2774); 10. *Crucella euganea* (Squinabol, 1903) (INV 2019.2775); 11. *Crucella* sp. 1 (INV 2019.2776); 12. *Crucella* sp. 2 (INV 2019.2777); 13. *Paronaella* sp. cf. *P. communis* (Squinabol, 1903) (INV 2019.2778); 14.*Halesium* sp. cf. *H. nevianii* (Squinabol, 1903) (INV 2019.2779.1) 15-16.*Halesium* sp. cf. *H.. crassum* (Ozvoldová, 1979) (INV 2019.2779.2 and INV 2019.2779.3); Scale bars are in μ. All illustrated specimens were extracted from the Shuru section of the Dumak ophiolite mélange, Eastern Iran

Figure 6 1-2. *Archaeospongoprunum cortinaense* Pessagno, 1973 (INV 2019.2780.1 and INV 2019.2780.2); 3. *Becus* sp. cf. *B. gemmatus* Wu, 1986 (INV 2019.2781); 4-5. *Dactyliodiscus cayeuxi* Squinabol, 1903 (INV 2019.2782.1 and INV 2019.2782.2); 6. *Dactyliodiscus* sp. cf. *D. longispinus* (Squinabol, 1904) (INV 2019.2783); 7. *Becus* sp. cf. *B. gemmatus* Wu, 1986 (INV 2019.2786); 8-9. *Acanthocircus levis* (Donofrio and Mostler, 1978) (INV 2019.2784.1 and INV 2019.2784.2); 10. *Acanthocircus multidentatus* (Squinabol, 1914) (INV 2019.2785); 11-12. *Napora crassispina* (Squinabol, 1903) (INV 2019.2787.1 and INV 2019.2787.2); 13-14. *Napora* sp. (INV 2019.2788.1 és INV 2019.2788.2); 15. *Sciadiocapsa* sp. (INV 2019.2789); 16. *Archaeodictyomitra chalilovi* (Aliev, 1965) (INV 2019.2790); 17-18. *Archaeodictyomitra vulgaris* Pessagno, 1977 (INV 2019.2791.1 and INV 2019.2791.2); 19. *Thanarla brouweri* (Tan, 1927) (INV 2019.2792). Scale bars are in μ. All illustrated specimens were extracted from the Shuru section of the Dumak ophiolite mélange, Eastern Iran

Figure 7 1-2. *Dictyomitra gracilis* (Squinabol, 1903) (INV 2019.2793.1 and INV 2019.2793.2) 3-5. *Dictyomitra montisserei* (Squinabol, 1903) (INV 2019.2794.1-3); 6-8. *Dictyomitra obesa* (Squinabol, 1903) (INV 2019.2796.1-3); 9. *Dictyomitra* sp. cf. *D. obesa* (Squinabol, 1903) (INV 2019.2797); 10-11. *Pseudodictyomitra lodogaensis* Pessagno, 1977b (INV 2019.2799.1 and INV 2019.2799.2); 12. *Obeliscoites perspicuus* (Squinabol, 1903) (INV 2019.2798); 13-14. *Pseudodictyomitra lodogaensis* Pessagno, 1977b (INV 2019.2799.3); 15-16. *Pseudodictyomitra* sp. cf. *P. lodogaensis* Pessagno, 1977b (INV 2019.2800.1-3). Scale bars are in μ. All illustrated specimens were extracted from the Shuru section of the Dumak ophiolite mélange, Eastern Iran.

Figure 8 1-2. *Xitus mclaughlini* (Pessagno, 1977b) (INV 2019.2801.1 and INV 2019.2801.2); 3. *Xitus spinosus* (Squinabol, 1904) (INV 2019.2802); 4. *Xitus* sp. cf. *X. spineus* Pessagno, 1977 (INV 2019.2803); 5-6. *Parvimitrella communis* (Squinabol, 1903) (INV 2019.2804.1, INV 2019.2804.2); 7. *Xitus subitus* Vishnevskaya, 1991 (INV 2019.2813) 8. *Xitus* sp. (INV 2019.2805); 9. *Parvimitrella* sp. (INV 2019.2806); 10. *Parvimitrella magna* Squinabol, 1904 (INV 2019.2807); 11-12. *Dorypyle communis* (Squinabol, 1903) (INV 2019.2808.1 and INV 2019.2808.2); 13-14. *Squinabollum fossile* (Squinabol, 1903) (INV 2019.2809); 15-16. *Crococapsa asseni* (Tan, 1927) (INV 2019.2810.1 and INV 2019.2810.2); 17. *Hiscocapsa grutterinki* (Tan, 1927) (INV 2019.2811); 18. *Crococapsa* sp. (INV 2019.2812). Scale bars are in μ. All illustrated specimens were extracted from the Shuru section of the Dumak ophiolite mélange, Eastern Iran.

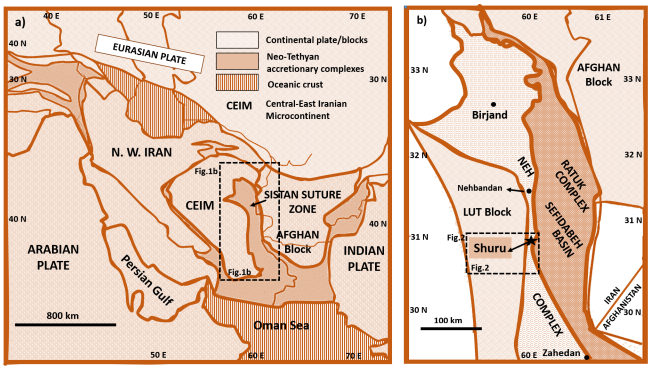

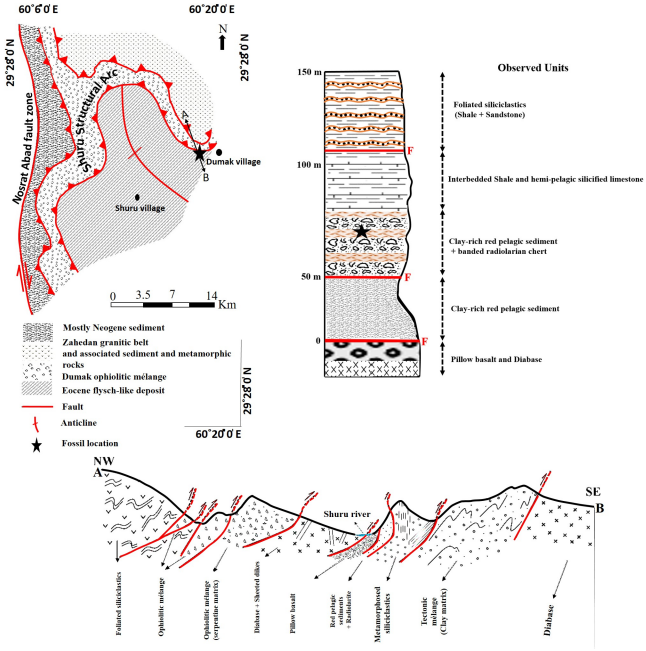

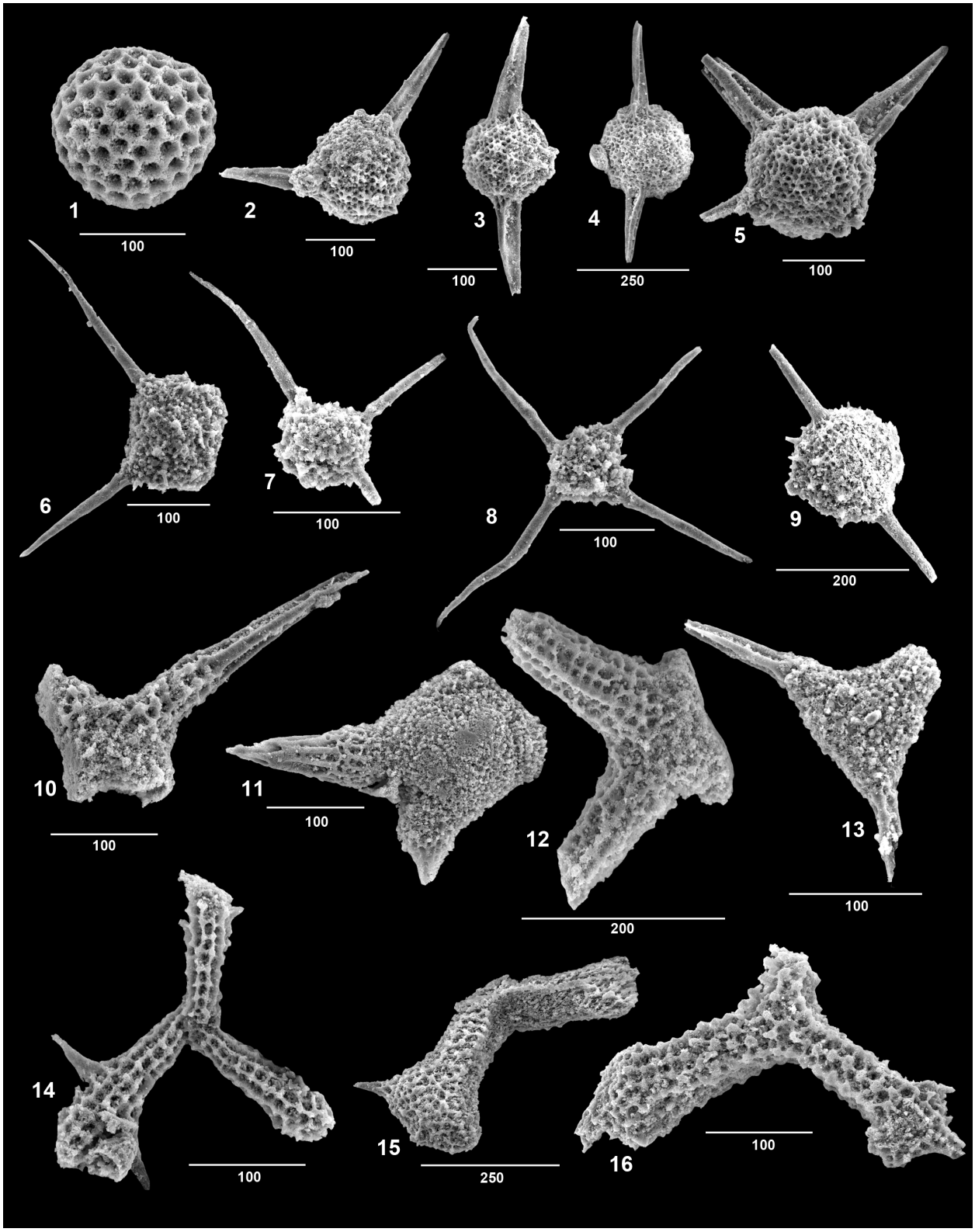
1
100
2
100
3
100
4
250
5
100
6
100
7
100
8
100
9
200
10
100
11
100
12
200
13
100
14
100
15
250
16
100

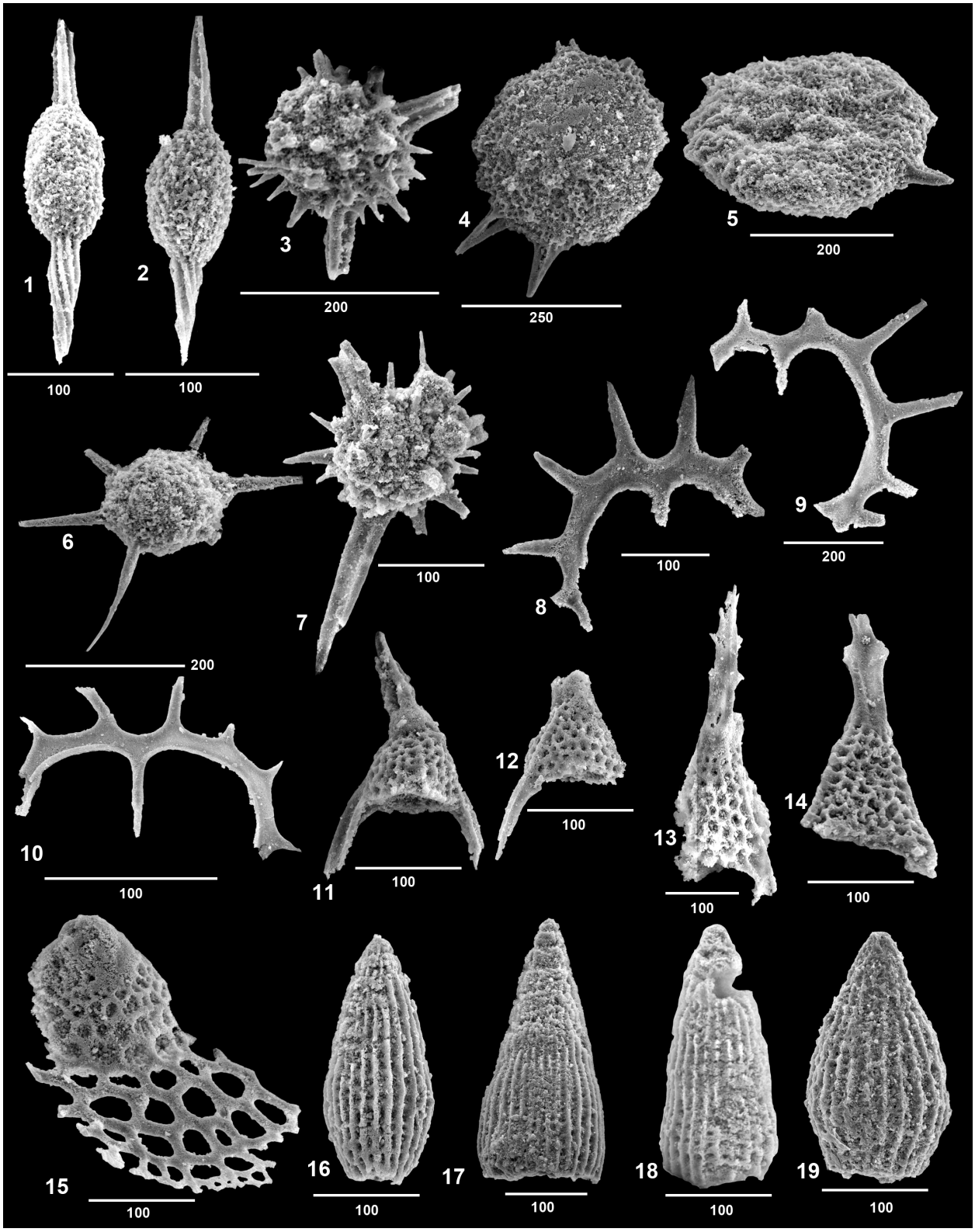
1
100
2
100
3
200
4
250
5
200
6
200
7
100
8
100
9
200
10
100
11
100
12
100
13
100
14
100
15
100
16
100
17
100
18
100
19
100

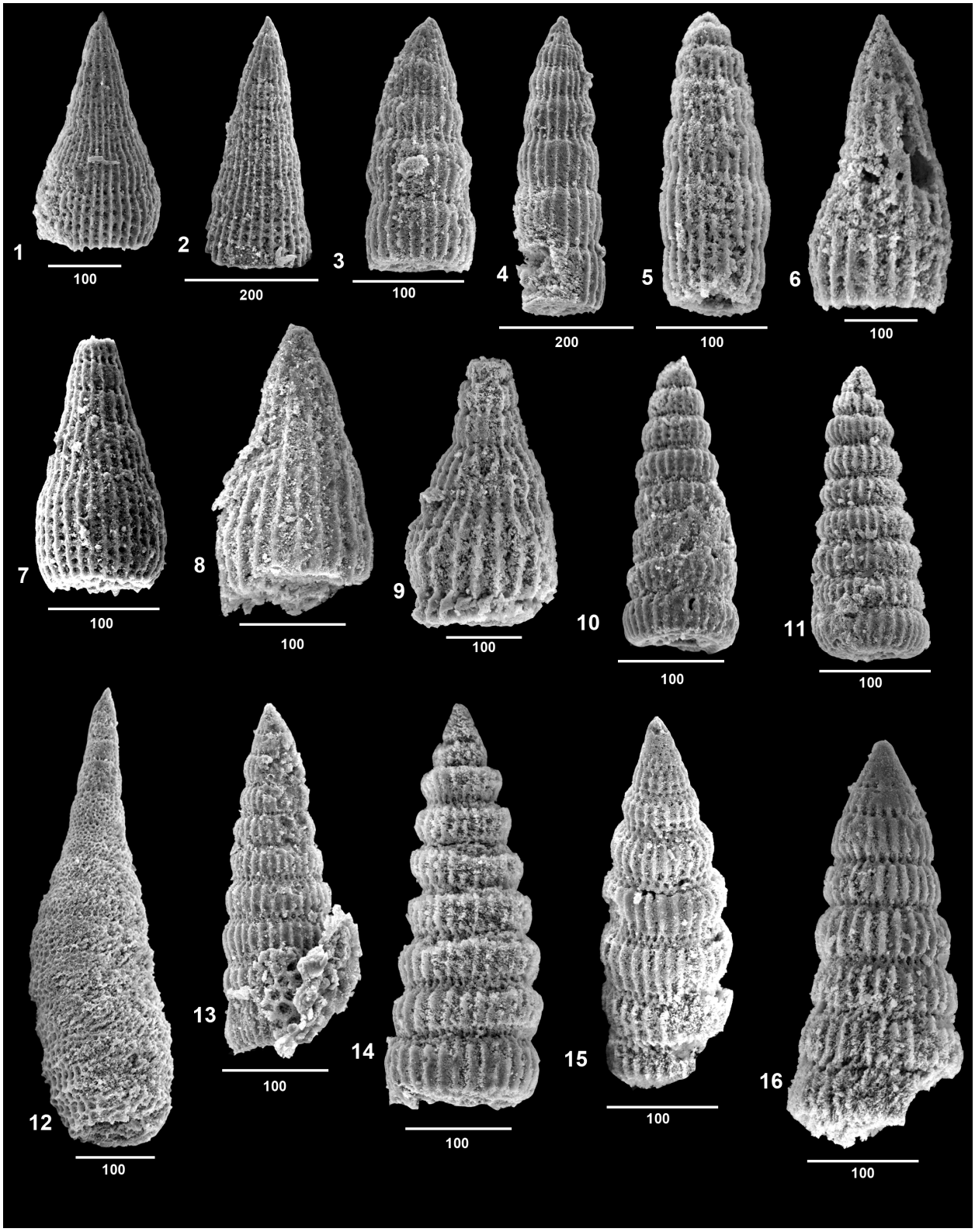
1
100
2
200
3
100
4
200
5
100
6
100
7
100
8
100
9
100
10
100
11
100
12
100
13
100
14
100
15
100
16
100

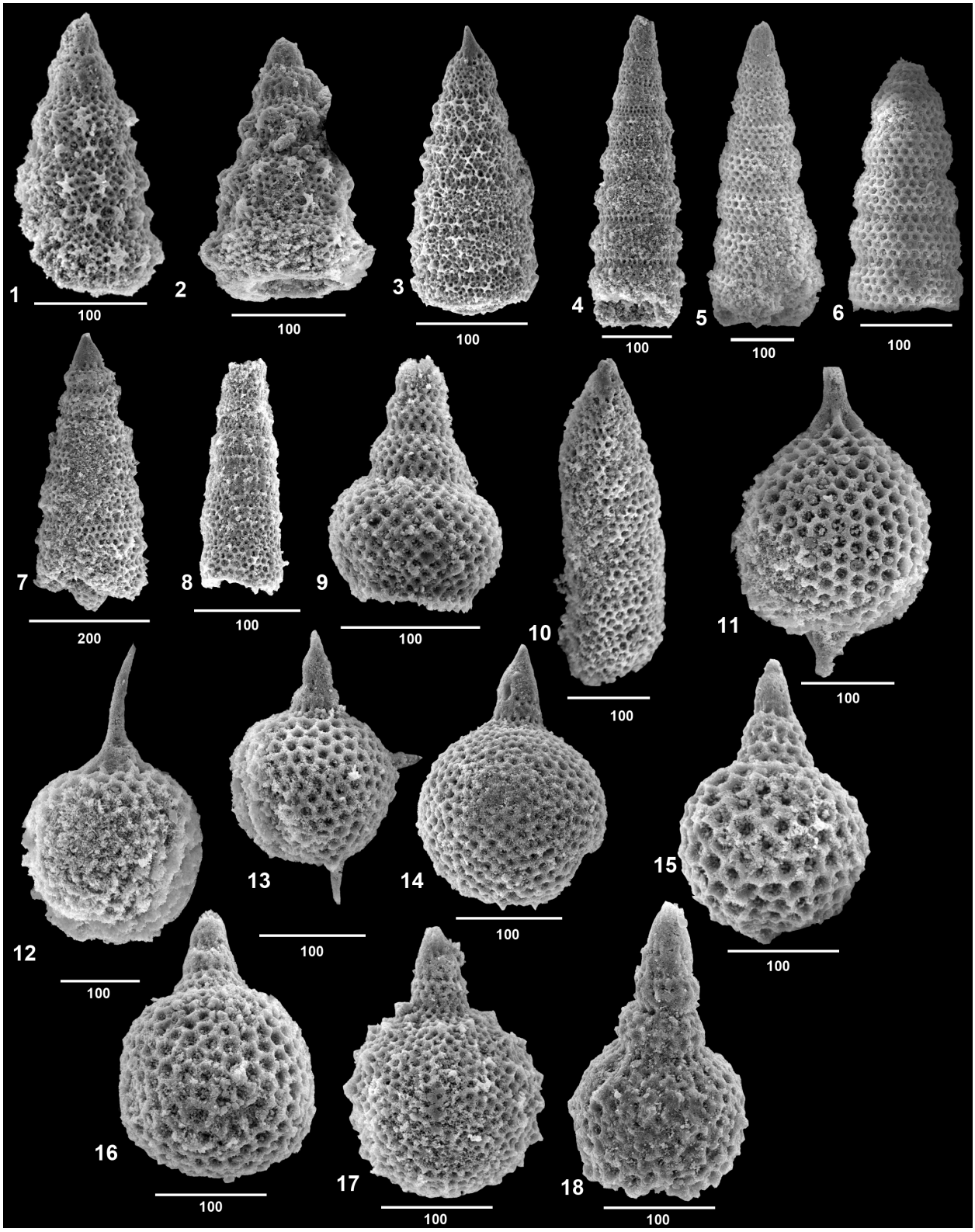
1
100
2
100
3
100
4
100
5
100
6
100
7
200
8
100
9
100
10
100
11
100
12
100
13
100
14
100
15
100
16
100
17
100
18
100

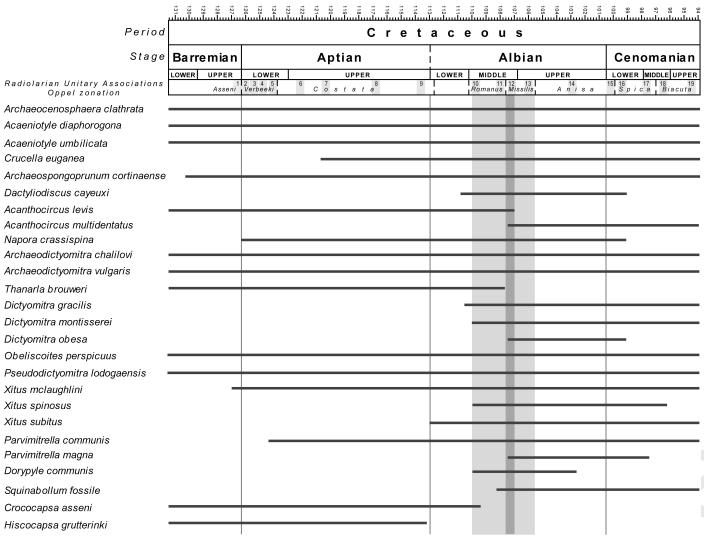

AUTHORSHIP STATEMENT

Manuscript title and authors: **New Albian (Cretaceous) radiolarian age data from the Dumak ophiolitic mélange in Shuru area, Eastern Iran** by P. Ozsvárt, E. Bahramnejad, S. Bagheri and M. Sharifi

All authors certify that they have participated sufficiently in the work to take public responsibility for the content, including participation in the concept, design, analysis, writing, or revision of the manuscript. Furthermore, each author certifies that this material or similar material has not been and will not be submitted to or published in any other publication before its appearance in the *Cretaceous Research*.

Conception and design of study: P. Ozsvárt, E. Bahramnejad, S. Bagheri

Sampling: E. Bahramnejad, S. Bagheri, M. Sharifi

Methodology: P. Ozsvárt, E. Bahramnejad, S. Bagheri, M. Sharifi

Investigation: P. Ozsvárt

Geological background: E. Bahramnejad, S. Bagheri, M. Sharifi

Resources: P. Ozsvárt

Interpretation: P. Ozsvárt

Writing - Original Draft: P. Ozsvárt, E. Bahramnejad, S. Bagheri, M. Sharifi

Writing - Review & Editing: P. Ozsvárt, E. Bahramnejad, S. Bagheri, M. Sharifi

Visualization: P. Ozsvárt, E. Bahramnejad

Author's name	Author's signature	Date
Péter Ozsvárt		13.01.2020
Elham Bahramnejad		13.01.2020
Sasan Bagheri		13.01.2020
Mortaza Sharifi		13.01.2020

Declaration of interests

☒ The authors declare that they have no known competing financial interests or personal relationships that could have appeared to influence the work reported in this paper.

☐The authors declare the following financial interests/personal relationships which may be considered as potential competing interests: